Co-targeting myelin inhibitors and CSPGs markedly enhances regeneration of GDNF-stimulated, but not conditioning-lesioned, sensory axons into the spinal cord

Jinbin Zhai, Hyukmin Kim, Seung Baek Han, Meredith Manire, Rachel Yoo, Shuhuan Pang, George M. Smith and Young-Jin Son*

Shriners Hospitals Pediatric Research Center and Center for Neural Repair and Rehabilitation, Lewis Katz School of Medicine, Temple University, Philadelphia, PA 19140

* Corresponding author: Young-Jin Son, PhD
Tel: (215) 926-9354
Email: yson@temple.edu

ABSTRACT

A major barrier to intraspinal regeneration after dorsal root (DR) injury is the DR entry zone (DREZ), the CNS/PNS interface. DR axons stop regenerating at the DREZ, even if regenerative capacity is increased by a nerve conditioning lesion. This potent blockade has long been attributed to myelin-associated inhibitors and CSPGs, but incomplete lesions and conflicting reports have prevented conclusive agreement. Here we evaluated DR regeneration in mice, using novel strategies to facilitate complete lesions and analyses, selective tracing of proprioceptive and mechanoreceptive axons, and the first simultaneous targeting of Nogo/Reticulon-4, MAG, OMgp, CSPGs and GDNF. Co-eliminating myelin inhibitors and CSPGs elicited regeneration of only a few conditioning-lesioned DR axons across the DREZ. Their absence, however, markedly and synergistically enhanced regeneration of GDNF-stimulated axons, highlighting the importance of sufficiently elevating intrinsic growth capacity. We also conclude that myelin inhibitors and CSPGs are not the primary mechanism stopping axons at the DREZ.

INTRODUCTION

The dorsal root (DR) carries primary sensory axons that project centrally from dorsal root ganglion (DRG) neurons to secondary neurons within the spinal cord and brainstem. DR injuries commonly result from brachial plexus, lumbosacral plexus and cauda equina trauma, and may cause permanent loss of sensation, uncoordinated movement and chronic pain (Carlstedt, 2008; Kaiser et al., 2020). The devastating consequences are because DR axons stop regenerating at the entrance of the spinal cord, the dorsal root entry zone (DREZ), and thus fail to restore connections with secondary neurons. Animal studies have reported functional recovery of nociception (Ramer et al., 2000; Romero et al., 2001; Cafferty et al., 2007; Liu et al., 2009; Lin et al., 2014; Kelamangalath et al., 2015), and, less frequently, of proprioception and mechanoreception (e.g., Wang et al., 2008; Cheah et al., 2016), for which large-diameter, myelinated proprio-/mechanoreceptive axons must regenerate far longer distances after crossing the DREZ.

Both neuron-intrinsic and extrinsic inhibitors, which limit axon regrowth elsewhere in the injured CNS (O'Shea et al., 2017; Griffin and Bradke, 2020), are widely thought to block regeneration at the DREZ. Notably, however, unlike direct CNS injury, DR injury damages

axons in the PNS without causing an impassable glial scar. Nevertheless, DR axons regenerating along the root quickly stop at the scar-free DREZ, even after a nerve conditioning lesion (Chong et al., 1999; Zhang et al., 2007; Di Maio et al., 2011). This potent blockade is surprising because a nerve conditioning lesion sufficiently enhances the growth potential of a limited number of dorsal column (DC) axons to penetrate a glial scar after spinal cord injury (Neumann and Woolf, 1999; Kwon et al., 2015). Why the scar-free DREZ is impenetrable even to conditioning lesioned axons remains unclear, but myelin-associated inhibitors and extracellular matrix-associated chondroitin sulfate proteoglycans (CSPGs) are conventionally considered responsible (Smith et al., 2012; Mar et al., 2016). This view is based on reports that individually targeting myelin inhibitors or CSPGs produced robust regeneration of DR axons, including proprio-/mechanoreceptive axons, across the DREZ. Soluble peptides blocking interactions between myelin inhibitors and Nogo receptors were observed to dramatically enhance robust functional regeneration of myelinated, but not unmyelinated, axons after DR crush (Harvey et al., 2009; Peng et al., 2010). Similarly, blocking PTPσ, a CSPG receptor, was reported to produce functional regeneration of myelinated DR axons into the spinal cord (Yao et al., 2019). Activating integrins has been found to elicit long-distance, topographic and functional regeneration of both myelinated and unmyelinated DR axons, presumably by counteracting myelin inhibitors, CSPGs and tenascin-C (Tan et al., 2011; Cheah et al., 2016).

Incomplete lesions and conflicting results have also hampered conclusive agreement about the mechanism of growth inhibition at the DREZ, including about the primacy of myelin inhibitors and CSPGs. Although no published studies have contradicted the reports of robust regeneration after pharmacologically targeting myelin inhibitors, two groups have found that removing CSPGs alone enables only minimal penetration of DR axons through the DREZ (Steinmetz et al., 2005; Wu et al., 2016). CSPG removal, however, when combined with conditioning lesions, neurotrophic factors or inflammation, has significantly enhanced intraspinal regeneration of DR axons (Steinmetz et al., 2005; Wu et al., 2016; Guo et al., 2019). Why eliminating CSPGs alone or a nerve conditioning lesion elicits only minimal regeneration across the DREZ is unknown, but the default assumption has been that myelin inhibitors alone are sufficiently potent to stop axons at the DREZ (Smith et al., 2012).

In the present work, we selectively traced regenerating proprio-/mechanoreceptive axons and used a novel wholemount assay to ensure that DR lesions were complete and the analysis comprehensive. Our analysis of triple knockout (tKO) mice lacking Nogo (A, B, C) (also known as Reticulon 4), MAG (Myelin-associated glycoprotein) and OMgp/Omg (Oligodendrocyte myelin glycoprotein), which is the first to genetically target all three major myelin inhibitors simultaneously, revealed that regeneration across the DREZ is not enhanced. Additionally, we found that supplemental removal of CSPGs in *Rtn4/Mag/Omg* tKO mice, the first combinatorial study to simultaneously eliminate myelin inhibitors and CSPGs, only modestly enhances regeneration of even conditioning lesioned DR axons. Thus, in contrast to the default assumption, which represents the prevalent view in the field, neither myelin inhibitors nor CSPGs, by themselves or even together, are sufficiently potent to prevent most DR axons from regenerating across the DREZ. Their absence, however, markedly and synergistically enhances intraspinal regeneration of GDNF-stimulated DR axons. These findings suggest the presence of inhibitory mechanism(s) of remarkably greater potency that potently blocks most axons at the DREZ, and that targeting myelin inhibitors and CSPGs can markedly enhance intraspinal penetration only when combined with an intervention that elevates axon growth capacity sufficiently robustly, above that achieved by a nerve conditioning lesion.

RESULTS

Intraganglionic AAV2-GFP selectively labels proprioceptive and mechanoreceptive axons

Conventional assessment of DR regeneration has relied heavily on immunolabeling of tissue sections and consequently was subject to labeling artifacts and limited sensitivity. We initiated the present study by identifying a viral tracer that intensely and reliably labels regenerating DR axons. We tested various recombinant viral vectors carrying fluorescent reporters by microinjecting them into cervical DRGs of uninjured adult mice. Of those we examined at 2 weeks post-injection, AAV2-GFP (self-complementary adeno-associated virus serotype 2-enhanced green fluorescent protein) almost exclusively transduced neurons, revealing brightly labeled cell bodies and axons (Figure 1A). After optimizing the virus titer, dosage, and microinjection technique, we were able to infect >70% neurons in most injections of DRGs (Figure 1B). Infected neurons included the three broadly classified subtypes of DRG neurons: large, neurofilament (NF)+ neurons, small- and medium sized IB4+ non-peptidergic neurons and

small CGRP+ peptidergic neurons (Figure 1C). Notably, a majority of the transduced, GFP-expressing neurons were NF+ (Figure 1D). In contrast, IB4+ neurons rarely were GFP+ and ~30% of GFP+ neurons were CGRP+ (Figure 1D), indicating that NF+ neurons were disproportionately transduced by AAV2-GFP. Consistent with the preferential infection of NF+ neurons, brightly labeled, large-diameter axons projected into the deeper layers of the dorsal horn (layer III-V) and into ventral horn, where large, myelinated axons terminate (Figure 1E). In contrast, superficial laminae of the dorsal horn, where small diameter unmyelinated axons terminate (layer I, II), lacked GFP fluorescence (Figure 1E' and E"), showing that AAV-GFP labels few if any IB4+ and CGRP+ axons. These findings are the first demonstration that AAV2-GFP predominantly transduces NF+ neurons and selectively reveals their proprio-/mechanoreceptive axons within the spinal cord.

NF+ neurons extend large-diameter myelinated axons that relay proprioception or mechanoreception via second order neurons located deep in the spinal cord and in distant dorsal column nuclei in the medulla (Niu et al., 2013). In contrast, IB4+ and CGRP+ neurons relay nociception through small-diameter unmyelinated axons that innervate secondary neurons in the superficial dorsal horn. Therefore, proprio-/mechanoreceptive axons require far more robust long-distance regeneration than nociceptive axons for functional recovery. Moreover, myelinated proprio-/mechanoreceptive axons regenerate more poorly than nonmyelinated nociceptive axons (Tessler et al., 1988; Guseva and Chelyshev, 2006; Han et al., 2017). Therefore, AAV2-GFP provides a unique opportunity to study selective regeneration of proprio-/mechanoreceptive axons whose regenerative capacity is particularly weak and needs robust augmentation.

Strategies for complete lesions and comprehensive evaluation of DR regeneration

Regeneration studies in animals suffer from conflicting and non-reproducible results, in part due to incomplete lesions which lead to mistakenly interpreting spared axons as regenerating axons (Steward et al., 2003; Steward et al., 2012). Completely crushing a DR is particularly demanding because DRs are tightly attached to spinal cord surfaces in flat, transparent layers (Han et al., 2012; Son, 2015). Various surgical methods have been applied to facilitate complete lesions, such as repetitive and bidirectional crushing of a root (Romero et al., 2001; Steinmetz et al., 2005;

Wu et al., 2016). However, there have been no assays that would confirm that a nerve crush surgery was successful.

We used two strategies to avoid spared axons. In one, we first crushed DRs and then micro-injected AAV2-GFP into DRGs (Figure 2A). This strategy transduces only axons proximal to the lesion, leading to labeling of regenerating, but not degenerating, distal stump axons. This is important because distal axons are very slowly removed in the CNS (Vargas and Barres, 2007), and thus can be mistakenly identified as regenerating axons in a conventional immunostaining analysis of transverse sections. In the second strategy, after euthanizing a mouse typically at 2 weeks post injury (wpi), we harvested spinal cords with attached DRs and DRGs, examined them first in wholemounts and excluded those with poor viral infections. We then carefully examined the properly labeled wholemounts and confirmed that lesions were complete (e.g., Figure 2B). We excluded those containing spared axons with the following characteristics: present in groups of only a few, relatively straight and extremely lengthy processes that extend along the entire length of the spinal cord and terminate with no discernable axon endings (e.g., Figure 2C; Han et al., 2012). A highly experienced surgeon performed all the root crushes. Nevertheless, incomplete lesions occurred in ~20% of the animals, typically because axons had been spared in the outermost dorsal rootlets (Figure 2C).

The wholemounts also enabled us to examine an unprecedented number of regenerating proprio-/mechanoreceptive axons from multiple injured roots. After a complete root crush in a wildtype (WT) mouse, hundreds of GFP+ axons all terminated at similar locations along the length of the dorsolateral spinal cord (Figure 2B, Figure 2-figure supplement 1). These GFP+ axons crossed the astrocyte: PNS border marked by GFAP (dotted lines) and terminated mostly within ~200μm of the border, forming a narrow front of axon tips (Figure 2D). Following wholemount assessment, we prepared serial transverse sections and evaluated regeneration of DR axons, across the DREZ and within the spinal cord. In WT mice, axons frequently grew dorsally along the growth-permissive pia matter (Figure 2E; arrowheads). We occasionally observed axons located subdurally several hundred microns past the astrocyte: PNS border (Figure 2E; arrow). Most axons, however, were located within ~100μm of the border and only a few axons reached ~200μm (Figure 2F). In the present comparative analyses, we considered axons that grew farther

than 100μm from the border as having penetrated the DREZ (Figure 2F). When astrocytes could not be co-immunostained, the astrocyte:PNS border was identified by DAPI staining of cell nuclei that accumulate much more densely in the PNS than CNS. The borders delineated by GFAP and DAPI overlap closely with each other (Figure 2E). DAPI also delineate boundaries closely overlapped with those identified by laminin (Figure 2-figure supplement 2; see also Figure 6-figure supplement 1), another marker of the CNS:PNS border (Ramer et al., 2004; Hoeber et al., 2017), validating further our use of DAPI as an alternative boundary marker.

Genetic deletion of Nogo, MAG and OMgp elicits little regeneration across the DREZ

We first investigated the effects of simultaneous genetic deletion of myelin-associated inhibitors by examining global tKO mice lacking Nogo/Reticulon-4 isoforms (A, B, C), MAG and OMgp. These mice were initially raised on a mixed background, extensively characterized, and used to study spinal cord regeneration (Lee et al., 2010). Our examination of these non-congenic tKO mutants revealed no enhanced regeneration of DR axons across the DREZ (data not shown). To overcome possible complications due to genetic background (Montagutelli, 2000; Tedeschi et al., 2017), we subsequently obtained *Rtn4/Omg* double KO and *Mag* KO mice raised on a C57BL/6 background and bred them to generate congenic *Rtn4/Mag/Omg* tKO mice (Figure 3A). Congenic tKO mice were viable and fertile, with no gross abnormalities. They were intercrossed to generate additional 2–3-month-old tKO mice; age matched C57BL/6 mice were used as controls.

To examine DR regeneration, we unilaterally crushed L4 and L5 DRs ~3-5 mm from the DREZ and then microinjected high-titer AAV2-GFP into the ipsilateral L4 and L5 DRGs (Figure 3B). In this crush injury model, proximal axons of large, NF+ neurons are capable of regenerating across the injury site and growing along the root at ~1.5 mm/day until they are rapidly immobilized at the DREZ, ~4 days post injury (Di Maio et al., 2011). We examined WT and tKO at 2 wpi, which provides axons sufficient time to penetrate the DREZ if they are competent to do so. Wholemount examination of *Rtn4/Mag/Omg* tKO mice revealed many brightly labeled axons that extended along the L4 and L5 roots (Figure 3D), as they did also in WT mice (Figure 2B, 3C). In both tKO and WT mice, however, most GFP+ axons terminated at similar longitudinal locations near the astrocyte:PNS border. Some axons extended substantially longer

processes dorsally toward the spinal cord midline (Figure 3D; arrows). However, similar axons were also frequent in WT (Figure 3C; arrows), and their incidence and length were not noticeably different in tKO and WT mice. We next examined serial transverse sections of L4 and L5 spinal cords prepared from tKO mice. No sections revealed GFP+ axons that crossed the DREZ and grew deep into the spinal cord. Most axons stopped at the DREZ, within ~100μm of the astrocyte: PNS border, as in WT (Figure 3E-3G). Axons that extended longer distances grew along the growth-permissive pia matter (Figure 3F; arrowheads), as in WT (Figure 2E, 3E). Thus, in contrast to the earlier studies that reported robust regeneration of DR axons after pharmacological targeting of myelin signaling, genetic elimination of three major myelin inhibitors did not enable GFP+ axons to cross the DREZ. These results suggest that inhibiting myelin inhibitors alone is not sufficient to induce regeneration of proprio-/mechanoreceptive axons across the DREZ.

Supplementary CSPG removal slightly increases regeneration across the DREZ in tKO mice

The limited regeneration across the DREZ in *Rtn4/Mag/Omg* tKO could be due to redundant inhibition by CSPGs that by themselves might be capable of arresting axons at the DREZ. Conversely, CSPG removal might induce only minimal regeneration (Steinmetz et al., 2005; Wu et al., 2016) due to redundant and potent inhibition by other inhibitors. To test this possibility, we attenuated CSPGs in *Rtn4/Mag/Omg* tKO using lentivirus encoding Chondroitinase ABC (LV-chABC) (Jin et al., 2011). ChABC promotes axon regrowth by digesting growth-inhibitory glycosaminoglycan (GAG) chains on CSPGs (Muir et al., 2019). We unilaterally crushed L4 and L5 DRs of tKO mice, microinjected AAV2-GFP into the L4 and L5 DRGs, and injected high-titer LV-ChABC into the ipsilateral dorsal horn at multiple locations rostrocaudally along the L4-L5 DREZ (Figure 4A). Two weeks after injury, wholemounts of ChABC-expressed tKO mice appeared similar to those of WT mice: most GFP+ axons terminated near the astrocytic border (Figure 4B, 4C). We used CS56 antibody immunostaining to confirm that LV-ChABC effectively removed the inhibitory sulfated GAG chains on CSPGs (Figure 4E). Consistent with previous observations (Han et al., 2017), CSPG degradation was restricted to the dorsal horn on the injected side of the spinal cord (Figure 4E; asterisks). Notably, CSPGs were rapidly and markedly upregulated in Schwann cells after DR crush, resulting in far brighter CS-56

immunoreactivity in the PNS than in the CNS (data not shown). We observed considerable CS-56 immunoreactivity associated with Schwann cells near the DREZ in ChABC-expressed tKO mice (Figure 4E'; arrowheads). However, the intensity of immunoreactivity was markedly reduced compared to that in non-treated tKO mice, further suggesting that CSPGs at the DREZ were markedly attenuated by LV-ChABC.

Most of the serial transverse sections of L4 and L5 DREZ also showed DR axons arrested at the DREZ and were virtually indistinguishable from those of WT mice (Figure 4D, 4E). Some sections exhibited a few GFP+ axons located slightly deeper in the dorsal funiculus; such axons were not observed in WT or tKO (Figure 4E'; arrows). The number of axons at the DREZ was slightly increased in tKO compared to WT, as measured at 100μm past the astrocyte:PNS border (Figure 4F), presumably reflecting locally enhanced axon outgrowth following degradation of endoneurial CSPGs at or near the DREZ (Zuo et al., 1998; Graham and Muir, 2016). Those axons that extended across the DREZ were within 200μm of the astrocyte:PNS border and constituted only ~10% of GFP+ axons (Figure 4F), however, suggesting that additional attenuation of CSPGs in *Rtn4/Mag/Omg* tKO only modestly promoted regeneration across the DREZ. Thus, these findings, based on the first simultaneous targeting of myelin inhibitors and CSPGs, indicate that the limited regeneration in the absence of myelin inhibitors is unlikely because of CSPGs that by themselves might be capable of arresting most axons at the DREZ.

Chronic regeneration failure at the DREZ despite absence of Nogo/MAG/OMgp and CSPGs

Concurrent ablation of myelin inhibitors and CSPGs only slightly enhanced regeneration, as assessed at 2 wpi, enabling only ~10% GFP+ axons to reach intraspinally ~100μm past the DREZ. Additional axons may continue to penetrate the DREZ and grow within the spinal cord lacking myelin inhibitors and CSPGs. To investigate this possibility and the chronic effects of targeting myelin inhibitors and CSPGs, we next examined WT, *Rtn4/Mag/Omg* tKO and ChABC-expressed tKO mice at 4 wpi (Figure 5A). Consistent with earlier studies of WT mice that demonstrated rapid and persistent immobilization of DR axons at the DREZ (Golding et al., 1996; Di Maio et al., 2011), we observed no enhanced regeneration across the DREZ at 4 wpi in

WT mice, as examined in wholemounts (Figure 5B) or in transverse sections (Figure 5C). There was, however, a statistically insignificant increase in DR axons at the DREZ (Figure 5D).

Similarly, in *Rtn4/Mag/Omg* tKO at 4 wpi (Figure 5E, 5F, 5G), we found no qualitative or quantitative evidence that two additional weeks after injury enabled more axons to penetrate the DREZ. This finding suggests that DR axons were chronically immobilized as they entered the DREZ despite the absence of myelin inhibitors.

Likewise, ChABC-expressed *Rtn4/Mag/Omg* tKO mice exhibited little or no enhanced regeneration at 4 wpi, as examined in wholemounts (Figure 5H) and transverse sections (Figure 5I) (see also Figure 2-figure supplement 1). We observed no increase in GFP+ axons that crossed the DREZ, indicating that no additional axons penetrated the DREZ and that those axons intraspinally located at 2 wpi (~10% GFP+ axons) did not extend further within the spinal cord lacking CSPGs. We observed significantly more axons at the DREZ in ChABC-expressed *Rtn4/Mag/Omg* tKO mice at 4 wpi than at 2 wpi (Figure 5J) or than in WT or *Rtn4/Mag/Omg* tKO mice at 4 wpi (Figure 5K). Notably, however, these GFP+ axons remained at the DREZ, indicating that prolonged attenuation of CSPGs did not enable them to penetrate the DREZ lacking myelin inhibitors.

We also examined regeneration of CGRP+ nociceptive axons, which are not discernably labeled by AAV2-GFP. As anticipated, it was often not possible, as noted in WT mice at 2 wpi, to evaluate intraspinal regeneration on sections due to punctate residual CGRP immunoreactivity associated with superficial laminae of the ipsilateral dorsal horn, particularly in Lissauer's tract (Figure 2E: asterisks). Dorsal funiculus above the dorsal horn, however, largely lacked CGRP+ immunoreactivity, indicating little if any penetration of CGRP+ axons through the DREZ at 2 wpi in WT mice (Figure 2E). Similarly, dorsal funiculus lacked CGRP immunoreactivity at 4 wpi in WT (Figure 5C), *Rtn4/Mag/Omg* tKO (Figure 5F) and ChABC-expressed *Rtn4/Mag/Omg* tKO mice (Figure 5I). CGRP immunoreactivity in superficial laminae of these mice at 4 wpi appeared similar to that in WT mice at 2 wpi. Moreover, it was not directly connected to CGRP+ axons at the DREZ on any sections, indicating that no axons reached superficial laminae directly

through the DREZ. Thus, CGRP+ axons also stop at the DREZ even with concurrent prolonged absence of myelin inhibitors and CSPGs.

Collectively, these studies, which represent the first evaluation of DR regeneration in the prolonged and concurrent absence of myelin inhibitors and CSPGs, demonstrate that both myelinated and unmyelinated DR axons stop at the DREZ and continue to be immobilized, even if myelin inhibitors and CSPGs are simultaneously removed. Therefore, the minimal regeneration observed in earlier studies targeting CSPGs alone was not due to redundant inhibition by myelin inhibitors. Instead, our findings suggest that neither myelin inhibitors nor CSPGs, by themselves or even together, are sufficiently potent to prevent regeneration of most DR axons across the DREZ.

DR axons fail to penetrate the DREZ in *Rtn4/Mag/Omg* tKO even after a nerve conditioning lesion

Although genetic deletion of myelin inhibitors alone does not permit DR axons to grow through the DREZ, it may enable conditioned axons with enhanced growth capacity to do so. To test this possibility, we performed a single nerve crush conditioning lesion which alone fails to enhance regeneration across the DREZ (Chong et al., 1999; Zhang et al., 2007; Di Maio et al., 2011), by crushing the sciatic nerve 10 days before crushing the L4 and L5 roots (Figure 6A). At 2 wpi, wholemounts of GFP+ axons in conditioned *Rtn4/Mag/Omg* tKO mice did not show noticeably enhanced penetration of the DREZ (Figure 6C). Accordingly, serial transverse sections occasionally exhibited a few axons that reached dorsolateral grey matter (Figure 6E: arrow), but most GFP+ axons failed to penetrate the DREZ (Figure 6E, 6F). Dorsal funiculus lacked CGRP immunoreactivity, suggesting that conditioning lesioned CGRP+ axons also failed to penetrate the DREZ. Compared to WT and tKO mice (Figure 6F, see also Figure 2-figure supplement 1), conditioned tKO mice exhibited significantly more axons at the DREZ, presumably reflecting enhanced regeneration in the peripheral portion of the DR (Di Maio et al., 2011). We rarely observed axons extended more than >200μm from the astrocyte: PNS border in conditioned tKO mice, as in WT and non-conditioned tKO mice (Figure 6F). Therefore, removal of myelin inhibitors does not enable nerve crush conditioned axons to regenerate beyond the DREZ.

Double conditioning lesion modestly enhances regeneration of DR axons across the DREZ in WT mice

A single nerve crush does not provide maximal mechanical conditioning of DRG neurons. Neumann et al., observed that double conditioning lesions dramatically enhance regeneration of DC axons after spinal cord injury, presumably because the second nerve injury at 1 wpi sustains the enhanced growth capacity of DRG neurons (Neumann et al., 2005). Because the effects of double conditioning lesions on DR regeneration have not been studied, we investigated whether regeneration across the DREZ is enhanced. Following the double conditioning paradigm of Neumann et al., we transected the ipsilateral sciatic nerve 3 days before and 7 days after L4 and L5 DR crush in WT mice (Figure 6-figure supplement 1A). At 2 wpi, wholemounts of GFP+ axons in double lesioned WT mice did not show enhanced penetration of the DREZ (Figure 6-figure supplement 1D) compared to WT or tKO mice conditioned by a single nerve crush (Figure 6-figure supplement 1B, 1C). Notably, however, serial transverse sections frequently exhibited axons that entered dorsolateral grey matter (Figure 6-figure supplement 1G, 1H; arrows). Nonetheless, most GFP+ axons (>90%) failed to penetrate the DREZ and only a few reached 200μm beyond the DREZ (Figure 6-figure supplement 1J). Quantitative comparisons indicate that the double conditioning lesion enhanced regeneration in WT mice, to a level comparable to or slightly greater than a single crush conditioning lesion in *Rtn4/Mag/Omg* tKO mice (Figure 6-figure supplement 1J). However, it was far less efficacious than intraspinally expressed GDNF, which enabled many more GFP+ axons (>40%) to cross the DREZ and extend deeper in the spinal cord (Figure 6-figure supplement 1I, 1J; see also Figure 8D). Thus, like a single nerve crush conditioning lesion with supplementary removal of myelin inhibitors, a double conditioning lesion, although reported to markedly enhance regeneration of DC axons, failed to enable most DR axons to cross the DREZ after DR injury.

Supplementary CSPG removal minimally enhances regeneration of conditioning lesioned axons across the DREZ in tKO mice

We next asked whether additional attenuation of CSPGs in *Rtn4/Mag/Omg* tKO mice would enable robust penetration of conditioned axons through the DREZ. To test this possibility, we injected LV-ChABC rostrocaudally in dorsal horns along the L4-L5 DREZ in *Rtn4/Mag/Omg* tKO mice which received a single nerve crush conditioning lesion 10 days before crushing L4

and L5 roots (Figure 7A). Surprisingly, at 2 wpi, despite the concurrent degradation of CSPGs, conditioned axons of *Rtn4/Mag/Omg* tKO mice largely remained near the astrocyte:PNS border in wholemounts (Figure 7C, Figure 2-figure supplement 1). CS-56 antibody immunostaining confirmed effective removal of CSPGs in dorsal horns (Figure 7E; asterisk). Serial transverse sections occasionally revealed GFP+ axons that reached dorsolateral grey matter (Figure 7F; arrows), but most axons remained at the DREZ within ~100μm of the border (Figure 7G). Similarly, we observed no noticeably enhanced regeneration of CGRP+ axons in conditioned/ChABC-expressed *Rtn4/Mag/Omg* tKO (Figure 7F). These results demonstrate that additional removal of CSPGs did not enable significantly more GFP+ axons to penetrate the DREZ in conditioned tKO mice. In sum, CSPG degradation and/or a nerve conditioning lesion increases the number of axons at the DREZ in *Rtn4/Mag/Omg* tKO, but most axons (>90%) fail to extend across the DREZ (Figure 7H). CSPG removal improves penetration of conditioned or unconditioned axons in tKO mutant, but the effect is modest, enabling only ~10% axons to extend ~100μm past the DREZ (Figure 7H). These findings collectively suggest that the inhibitory role of myelin inhibitors and CSPGs at the DREZ, by themselves or even together, is moderate: they are not the primary factors that arrest even conditioning lesioned DR axons at the DREZ.

Nogo/MAG/OMgp removal markedly enhances intraspinal regeneration of GDNF-stimulated DR axons

Our findings that conditioning lesioned axons penetrate only modestly through the DREZ in ChABC-expressed tKO mice suggest that myelin inhibitors and CSPGs do not strongly inhibit DR axons. We also found that a double conditioning lesion fails to elicit robust DR regeneration, indicating that mechanical conditioning does not sufficiently enhance the intrinsic growth capacity of DR axons to cross the DREZ. If myelin inhibitors and CSPGs indeed play only a moderate inhibitory role at the DREZ, greater enhancement of intrinsic growth capacity may be essential for robust penetration in their absence. In addition, myelin inhibitors and CSPGs may hinder regeneration within the spinal cord, although their inhibition is insufficient to block most axons at the DREZ. To test further the efficacy of myelin inhibitors and CSPGs, we applied a treatment that enabled many axons to penetrate the DREZ and then examined if their intraspinal regeneration was altered in *Rtn4/Mag/Omg* tKO mice with or without additional attenuation of

CSPGs. Intraspinal expression of neurotrophic factors elevates regenerative capacity and chemotropically attracts DR axons, enabling them to cross the DREZ (Ramer et al., 2000; Iwakawa et al., 2001; Kelamangalath et al., 2015). When expressed virally within the spinal cord of WT mice, GDNF promoted penetration of many large-diameter DR axons through the DREZ and further into the spinal cord (Kelamangalath et al., 2015; Han et al., 2017).

We microinjected lentivirus expressing GDNF (LV-GDNF), extensively used in earlier studies (Deng et al., 2013; Zhang et al., 2013; Kelamangalath et al., 2015; Han et al., 2017), into the dorsal horn rostrocaudally along the L4-L5 DREZ at the time of DR crush in WT (Figure 8A) or *Rtn4/Mag/Omg* tKO mice (Figure 8E). At 2 wpi, wholemounts of GDNF-expressed WT mice did not show markedly enhanced regeneration into the spinal cord (Figure 8B). Serial sections, however, frequently revealed GFP+ axons that crossed the DREZ and extended further into the dorsal funiculus and grey matter (Figure 8C). Quantification indicated that ~50% of GFP+ axons penetrated the DREZ and extended up to ~300μm from the astrocyte:PNS border (Figure 8D). Consistent with an earlier study (Iwakawa et al., 2001), we also observed numerous CGRP+ axons in the dorsal funiculus, indicating regeneration of nociceptive axons across the DREZ in GDNF-expressed WT mice (Figure 8C).

Compared to GDNF-expressed WT mice, wholemounts of GDNF-expressed *Rtn4/Mag/Omg* tKO mice more frequently revealed areas of the DREZ that exhibited conspicuously intense GFP fluorescence, due to densely accumulated subdural GFP+ axons (Figure 8F, arrows; see also Figure 2-figure supplement 1). Indeed, serial sections often displayed abundant GFP+ axons at and beyond the DREZ, indicating markedly enhanced regeneration of GDNF-stimulated axons across the DREZ in tKO mice (Figure 8G). We also observed bright CGRP+ immunoreactivity in deep dorsal laminae which are usually devoid of residual CGRP+ staining, presumably indicating greatly enhanced regeneration of nociceptive axons in tKO mice (Figure 8G; asterisk). The number of axons that crossed the DREZ far exceeded that observed in GDNF-expressed WT mice, nearly tripling the number of GFP+ axons at 200μm from the astrocyte:PNS border (Figure 8H). Therefore, elimination of myelin inhibitors enabled many more GDNF-stimulated axons to extend across the DREZ. It was also notable that the number of axons crossing the DREZ at 100μm far exceeded the number of axons that entered the DREZ at 0μm (i.e., astrocyte:PNS

border) (Figure 8H). The number of intraspinal axons at 200μm was also significantly greater than the number of axons crossing the DREZ at 100μm. These findings suggest that elimination of myelin inhibitors enhanced intraspinal regeneration of GDNF-stimulated axons, largely by promoting regenerative sprouting or additional branch formation of parental axons at and beyond the DREZ.

Collectively, these findings indicate that myelin inhibitors are indeed inhibitory to DR axons and can restrict their regeneration at the DREZ and beyond it within the spinal cord. They also demonstrate that genetic elimination of myelin inhibitors alone or combined with a conditioning lesion promote minimal regeneration across the DREZ, reflecting their incomplete inhibitory effect. It can markedly enhance regeneration only in combination with a treatment that sufficiently enhances intrinsic growth capacity of DR axons.

CSPG removal further enhances intraspinal regeneration of GDNF-stimulated axons in tKO mice

Lastly, we investigated the synergistic effect of CSPG degradation on intraspinal regeneration of GDNF-stimulated axons in *Rtn4/Mag/Omg* tKO mice. We micro-injected LV-GDNF and LV-ChABC into dorsal horns and AAV2-GFP into DRGs at the time of L4 and L5 root crush (Figure 9A). At 2 wpi, wholemounts of GDNF/ChABC-expressed tKO mice revealed far broader areas of densely populated GFP+ axons growing into the CNS beyond the astrocyte:PNS border (Figure 9C; arrows) than in GDNF-expressed WT (Figure 9B; arrow) or in GDNF-expressed tKO mice (Figure 8F; see also Figure 2-figure supplement 1). Moreover, many GFP+ axons extended rostrocaudally close to the midline (Figure 9C; arrowheads), further evidence of enhanced intraspinal penetration and regeneration in GDNF/ChABC-expressed tKO mice. CS-56 antibody immunostaining confirmed effective removal of CSPGs in dorsal horns (Figure 9E). Serial transverse sections frequently showed GFP+ axons densely filling a broader and deeper area of the dorsal horn in GDNF/ChABC-expressed tKO mice (Figure 9E, 9F) than in GDNF-expressed WT (Figure 9D) or in GDNF-expressed tKO mice (Figure 8G; see also Figure 2-figure supplement 1). CGRP immunoreactivity on some sections was conspicuously bright, dense, and notably restricted to the superficial laminae, like CGRP immunoreactivity on the contralateral uninjured side (Figure 9F). Quantification indicated ~20% further increase in GFP+ axons

crossing the DREZ at 100μm, presumably reflecting enhanced regenerative sprouting, and ~60% increase in GFP+ axons at 400μm in deeper portions of the dorsal horn in GDNF/ChABC-expressed tKO mice, compared to GDNF-expressed tKO mice (Figure 9G). These findings show that additional removal of CSPGs markedly and synergistically enhanced regeneration of GDNF-stimulated axons across the DREZ in *Rtn4/Mag/Omg* tKO mice. Therefore, like myelin inhibitors, CSPGs partially restrict DR axons at and beyond the DREZ, and their removal can significantly enhance regeneration across the DREZ only when combined with an intervention that sufficiently enhances intrinsic growth capacity of DR axons.

DISCUSSION

Using novel multifaceted strategies, we directly compared DR regeneration in WT, *Rtn4/Mag/Omg* tKO, ChABC-expressed tKO, GDNF-expressed tKO and GDNF/ChABC-expressed tKO mice, either with or without a nerve conditioning lesion. Co-eliminating myelin inhibitors and CSPGs only slightly increased regeneration across the DREZ, surprisingly even after an additional conditioning lesion. Their absence, however, markedly and synergistically enhanced regeneration of GDNF-stimulated axons across and beyond the DREZ. These findings suggest the existence of a myelin/CSPG-independent mechanism that potently restrains most axons at the DREZ, and that this barrier can be overcome by elevating axon growth capacity, above that achieved by a nerve conditioning lesion. The results also suggest that therapeutically targeting both myelin inhibitors and CSPGs can enhance, but will not induce, regeneration of most DR axons into the spinal cord.

Various AAV vectors, including AAV2, demonstrate neuronal tropism (Mason et al., 2010; Fischer et al., 2011). Several AAV serotypes exhibit differential tropism for specific subpopulations of DRG neurons: AAV6 preferentially transduces small-sized neurons; AAV5, 8, and 9, large neurons (Jacques et al., 2012; Yu et al., 2013; Wu et al., 2016; Kubota et al., 2019). We found that AAV2 preferentially transduces NF+ neurons. Approximately 80% of GFP+ neurons were NF+, although only ~50% of lumbar DRG neurons are NF+ in mice (Li et al., 2016). IB4+ neurons constituted only ~5% of GFP+ neurons while CGRP+ neurons accounted for ~30%. Because ~30% of CGRP+ neurons also express NF200 (Li et al., 2016), our results are likely an overestimation of CGRP+ neurons projecting nociceptive axons. GFP expression in

superficial dorsal laminae (I-IIi), where nociceptive afferents terminate, was almost undetectable (Figure 1E; arrow). It appears, therefore, that the predominant transduction of NF+ neurons and minimal expression of GFP in CGRP+ axons make AAV2-GFP a valuable tracer of proprioceptive and mechanoreceptive axons.

Axon sparing has hampered consistent and conclusive studies with the widely used DR crush model (Smith et al., 2012). We found that complete crushing is difficult even in fluorescent mice whose axons are well visualized. Furthermore, improperly crushed axons often recover connectivity with distal axons (Di Maio et al., 2011; Han et al., 2012). Here we studied L4-L5 roots because in our experience DR crush is more likely to spare cervical than lumbar roots. In addition, we used wholemount preparations to detect spared axons, which is possible because AAV2-GFP brightly labels numerous axons. Importantly, however, wholemount assessment does not guarantee complete lesions because viral transduction does not label all axons and spared axons that are deeply located may be overlooked.

Wholemounts also permitted simultaneous assessment of many axons in multiple roots, which has not been achieved previously. Greatly enhanced regeneration appeared as areas with unusually bright, dense GFP fluorescence. Rostrally extending bundles of GFP+ axons were also observed when intraspinal penetration exceeded 50%. These features require many intraspinally regenerating axons and therefore provide convincing evidence of robustly enhanced intraspinal penetration through the DREZ. Accordingly, wholemount assay is particularly useful for studies such as the present one, which uses a relatively small number of animals. We excluded mice for various reasons, including incomplete lesions and poor axon labeling, and used 3-8 mice per cohort to compare a total of 12 different animal groups. Nevertheless, no tKO, ChABC-expressed tKO, or conditioning lesioned/ChABC-expressed tKO mice exhibited either fluorescent areas of densely populated axons or rostral axon bundles. In contrast, these features were consistent findings in all the wholemounts of GDNF-expressed tKO and GDNF/ChABC-expressed tKO mice. Uniform absence or presence of these major features in wholemounts is therefore useful to determine if a specific factor serves as a major inhibitor or promoter of DR regeneration across the DREZ.

Our results suggest that myelin inhibitors and CSPGs play only a limited role in restraining axon outgrowth at the DREZ. For example, combined removal of these inhibitors enabled only about ~10% of axons to cross the DREZ and extend ~100μm beyond it. Prolonged elimination for a month after injury also did not increase intraspinal penetration. More surprisingly, GDNF elicited markedly enhanced intraspinal regeneration in the absence of myelin inhibitors and CSPGs, unlike nerve crush conditioning lesion that produced little enhancement. If myelin inhibitors and CSPGs played a dominant role in restraining axons at the DREZ, then removing them should be sufficient to drive vigorous penetration. If their contribution is limited, then greater enhancement of axon growth potential might be essential for robust penetration, as we observed with supplementary expression of GDNF.

It is unlikely that the limited enhancement with a conditioning lesion was due to insufficient removal of Nogo/MAG/OMgp or CSPGs. Most notably, GDNF robustly enhanced regeneration in tKO and produced even more intraspinal regeneration in ChABC-expressed tKO mice. These observations, together with earlier studies that demonstrated efficacy of the *Rtn4/Mag/Omg* tKO and LV-ChABC (Curinga et al., 2007; Lee et al., 2010; Jin et al., 2011; Han et al., 2017), indicate that penetration through the DREZ was not limited because of insufficient elimination of Nogo/Reticulon-4, MAG, OMgp, CSPGs and/or undigested CSPG carbohydrate stubs (Lemons et al., 2003). Our findings are consistent with earlier observations in WT mice that degrading CSPGs alone (Steinmetz et al., 2005; Wu et al., 2016), or in combination with conditioning lesions (Quaglia et al., 2008) elicits minimal intraspinal penetration. Importantly, our findings demonstrate for the first time that the minimal penetration elicited by the absence of CSPGs was highly unlikely due to synergistic restraint by myelin inhibitors.

Our findings contrast with the robust, long-distance functional regeneration of myelinated DR axons reported in earlier studies that pharmacologically targeted Nogo receptor or CSPG/CSPG receptors, with or without a nerve crush conditioning lesion (Harvey et al., 2009; Peng et al., 2010; Cheah et al., 2016; Yao et al., 2019). Blocking inhibitors in adulthood may be more effective than eliminating them during development due to compensatory upregulation of other inhibitors (El-Brolosy and Stainier, 2017). It is noteworthy, however, that we removed CSPGs in adult tKO mice. Another possible explanation for the discrepancy is a species difference between

mice and rats (Lee and Lee, 2013), but results have also conflicted in the same species. Additional myelin-associated inhibitors and ligands of Nogo and CSPG receptors have been identified (Zhang et al., 2009b; Dickendesher et al., 2012; Thiede-Stan and Schwab, 2015; Ohtake et al., 2018). However, CSPGs are the major additional ligands that bind to the Nogo receptor (Dickendesher et al., 2012), yet co-eliminating CSPGs and myelin inhibitors elicited little penetration through the DREZ. An alternative explanation is that these studies included incomplete lesions of varying extent, which were followed by acute or gradual functional recovery that did not require actual regeneration or relied on sprouting of spared axon terminals (Cafferty et al., 2008).

Myelin inhibitors and CSPGs are thought to stop axons at the DREZ by collapsing or trapping growth cones and inducing dystrophic endings (Li et al., 1996; Golding et al., 1999; Ramer et al., 2001; Tom et al., 2004; Smith et al., 2012). Our results revise this long-held view by suggesting the presence of inhibitory mechanism(s) of remarkably greater potency that act independently of myelin inhibitors and CSPGs. One such inhibitory mechanism may be the expression of additional repellent cues that are upregulated at the axotomized DREZ (Andrews et al., 2009; Lindholm et al., 2017). Another possibility is that most DR axons are stabilized at the DREZ by forming aberrant synapses rather than dystrophic endings with unknown postsynaptic cells (Carlstedt, 1985; Liuzzi and Lasek, 1987; Stensaas et al., 1987; Di Maio et al., 2011; Son, 2015). Consistent with this notion, DC axons form synapse-like endings on NG2+ cells following spinal cord injury (Busch et al., 2010; Filous et al., 2014). It remains to be determined whether NG2+ cells are postsynaptic cells at the DREZ, and whether all axons stop by forming aberrant synapses with NG2+ cells (Son, 2015). We could not examine this possibility in the present study because of the experimental challenges of differentiating dystrophic from synaptic endings, and in blocking aberrant synapse formation. Other possible, although less likely, mechanisms include lack of a growth-permissive/promoting substrate (Li et al., 2004; Han et al., 2017; Collins et al., 2019) and/or inadequate intrinsic growth ability of DRG neurons (Steinmetz et al., 2005; Nichols and Smith, 2020).

Targeting Nogo, CSPGs or their receptors in rodent models of spinal cord injury promotes minimal regeneration of myelinated axons, such as corticospinal tract (Fink et al., 2015; Lang et

al., 2015; Ito et al., 2018). However, their removal can significantly enhance the growth promotion of a combinatory treatment by stimulating sprouting (Wang et al., 2012; DePaul et al., 2017; Wu et al., 2017). Consistent with these observations after spinal cord injury, we found that eliminating myelin inhibitors alone or in combination with CSPG removal markedly enhanced intraspinal regeneration of GDNF-stimulated axons, largely by stimulating regenerative sprouting. Thus, their removal can allow robust intraspinal regeneration but only when combined with a treatment that sufficiently enhances axon growth capacity. We chose to enhance growth capacity with GDNF rather than with zymogen or caBRAF, which stimulated greater intraspinal penetration (Steinmetz et al., 2005; O'Donovan et al., 2014). We were concerned that excessive enhancement of intrinsic growth capacity might impede evaluating the efficacy of extrinsic growth inhibitors in arresting axons at the DREZ. In addition, we observed that zymogen administration causes DRG neurons progressively to die in mice, likely due to severe inflammation (Kim et al., unpublished), and that it is challenging to provide supplemental genetic conditioning of caBRAF in tKO.

A single sciatic nerve conditioning lesion of DRG neurons has been extensively used for epigenetic, transcriptomic and proteomic studies of peripheral and central regeneration (Blesch et al., 2012; Li et al., 2015; Palmisano et al., 2019). We found that a conditioning lesion does not sufficiently elevate axon growth capacity to overcome the potent myelin/CSPG-independent inhibitory mechanism(s). Furthermore, a double conditioning lesion only modestly enhances intraspinal regeneration in WT mice, to a level comparable to that found with a single crush lesion in tKO mice, but that even the double lesion was far less efficacious than GDNF in enabling axons to cross the DREZ. Therefore, more axons may be able to cross the DREZ when the double conditioning lesion is combined with co-eliminating myelin inhibitors and CSPGs, but we will expect to observe substantially fewer axons than when GDNF treatment is combined with co-eliminating these inhibitors. Although our results highlight the importance of sufficiently elevating axon growth capacity, GDNF enhanced penetration of ~40% DR axons in WT mice. Moreover, the intraspinal regeneration it elicited in the absence of myelin inhibitors and CSPGs was apparently enhanced but did not appear sufficiently robust to power the long-distance regeneration required for proprio-/mechanoreceptive axons. The DR regeneration induced by several other neurotrophic factors, cytokines and downstream effectors has been generally

weaker than that elicited by GDNF in ChABC-expressed tKO mice (O'Donovan et al., 2014; Liu et al., 2016; Wu et al., 2016). Learning therapeutically applicable treatment of maximizing axon growth capacity must be as important as understanding the myelin/CSPG-independent mechanism that powerfully halts axons at the DREZ, and perhaps also within the damaged spinal cord.

MATERIALS AND METHODS

Reagent type (species) or resource	**Designation**	**Source or Reference**	**Identifiers**	**Additional Information**
Strain, strain background (*Mus musculus*)	*Rtn4/Omg* double knockout	Dr. Binhai Zheng (UCSD)	RRID:MGI:3624445 RRID:MGI:3821705	Lee et al., 2010
Strain, strain background (*Mus musculus*)	*Mag* knockout	Dr. Jae K. Lee (U.Miami)	Stock #: 006865; RRID:IMSR JAX:006865	
Strain, strain background (*Mus musculus*)	C57BL/6J	The Jackson Laboratory	Stock #: 000664; RRID:IMSR JAX:000664	

Other	Vectashield	Vector Laboratories, Burlingame	H-100 RRID:AB2336789	mounting medium
transfected construct (*Mus musculus*)	scAAV2-eGFP	Dr. George M. Smith (Temple University)		AAV construct to transfect and express eGFP (Liu et al., 2014)
transfected construct (*Mus musculus*)	LV-chABC	Dr. George M. Smith (Temple University)		Lentiviral construct to transfect and express chABC (Curinga et al., 2007)
transfected construct (*Mus musculus*)	LV-GDNF	Dr. George M. Smith (Temple University)		Lentiviral construct to transfect and express GDNF (Zhang et al., 2013)
Antibody	anti-NF200 (rabbit polyclonal)	Sigma	#N4142 RRID:AB477272	IHC (1:500)
chemical compound, drug	Isolectin B4, biotin conjugate	Sigma	#L2140 RRID:AB2313663	IHC (1:200)

Antibody	anti-CGRP (rabbit polyclonal)	Peninsula Labs	#T4032 RRID:AB2307330	IHC (1:2,000)
Antibody	anti-GFP (mouse monoclonal)	Avés Labs Inc.	#GFP-1020 RRID:AB10000240	IHC (1:500)
Antibody	anti-GFAP (rabbit polyclonal)	Agilent	#N1506 RRID:AB10013482	IHC (1:500)
Antibody	Alexa Fluor 647-goat anti-rabbit IgG secondary antibody	Invitrogen	#31573 RRID:AB2536183	IHC (1:400)
Antibody	Fluorescein (FITC)-conjugated goat anti-rabbit IgG secondary antibody	Millipore	#AP307F RRID:AB92652	IHC (1:400)
Antibody	Alexa Fluor 568-conjugated goat anti-mouse IgG_1 secondary antibody	Invitrogen	# A21124 RRID:AB141611	IHC (1:400)
Antibody	rhodamine (TRITC)-conjugated	Jackson ImmunoResearch Labs Inc.	#016-020-084 RRID:AB2337237	IHC (1:400)

	streptavidin secondary antibody			
Antibody	Alexa-Fluor 568-conjugated goat anti-rabbit secondary antibody	Invitrogen	#A11011 RRID:AB143157	IHC (1:400)
Antibody	Alexa Fluor 488-donkey anti-chicken IgG secondary antibody	Jackson ImmunoResearch Labs Inc.	#703-545-155 RRID:AB2340375	IHC (1:400)
other	DAPI stain	Thermo Fisher Scientific	#D1306 RRID:AB2629482	IHC (1:1,000)
other	Nissl substance stain	Thermo Fisher Scientific	#N21482 RRID:AB2620170	IHC (1:200)
software, algorithm	MetaMorph Image Analysis Software	Molecular Devices	RRID:SCR002368	
software, algorithm	AxioVision Imaging System	Zeiss	RRID:SCR002677	
software, algorithm	Axio Imager	Zeiss	RRID:SCR018876	
software, algorithm	Imaris	Bitplane	RRID:SCR007370	

software, algorithm	Adobe Photoshop	Adobe Inc.	RRID:SCR014199	
software, algorithm	PRISM 8.0	GraphPad	RRID:SCR002798	

Mice. All animal care and procedures were conducted in accordance with the National Research Council's Guide for the Care and Use of Laboratory Animals and approved by the Institutional Animal Care and Use Committee at Lewis Katz School of Medicine at Temple University (animal protocol #4919), Philadelphia, PA, USA. Congenic *Rtn4/Mag/Omg* triple knockout mice were generated by breeding congenic lines of *Rtn4/Omg* double knockout mice obtained from Dr. Binhai Zheng (University of California at San Diego) and of MAG single knockout mice obtained from Dr. Jae K. Lee (University of Miami). Male and female, 2-3 months old $Rtn4^{-/-}/Omg^{-/-}/Mag^{-/-}$ mice and age-matched C57BL/6J mice (The Jackson Laboratory) were used. Mice were genotyped at the time of weaning by tail clipping and PCR analysis using the primers described in earlier studies (Li et al., 1994; Lee et al., 2010).

Dorsal root crush. Mice were anesthetized with an intraperitoneal injection of xylazine (8 mg/kg) and ketamine (120 mg/kg). Supplements were given during the procedure as needed. Following a 2- to 3-cm-long incision in the skin of the back, the spinal musculature was reflected and the L3–S1 spinal cord segments exposed by hemilaminectomies to prepare for unilateral L4–L5 root crush. The cavity made by the laminectomies was perfused with warm sterile Ringer's solution. A small incision was made in the dura overlying the L4 and L5 DR. A fine forceps (Dumont #5; Fine Science Tools, Foster City, CA) was introduced subdurally and the DR crushed for 10 s. To avoid scar formation and possible compression, we applied a piece of thin SILASTIC membrane (Biobrane, Bertek Pharmaceuticals, Sugarland, TX) over the laminectomy site and covered it with a layer of thicker artificial dura (Gore Preclude MVP Dura Substitute, W.L. Gore and Associates, Flagstaff, AZ). The overlying musculature was closed with 5-0 sutures, and the skin closed with wound clips. All animals received subcutaneous injections of saline (0.9% w/v NaCl) and buprenorphine (0.05 mg/kg) for postoperative pain management and remained on a heating pad until fully recovered from anesthesia. Mice were perfused 2 or 4 weeks after the crush, and

axon regeneration was analyzed in cryostat sections or in thin dorsal slice preparations of whole spinal cord.

Nerve conditioning lesion. DRG neurons were preconditioned by crushing the sciatic nerve in the lateral thigh of the ipsilateral hind leg 10 days before the DRs were crushed. Animals were anesthetized as described above; the skin and superficial muscle layer of the midthigh were opened; and the sciatic nerve was crushed for 10 s with fine forceps (Dumont #5; Fine Science Tools, Foster City, CA). The muscle and skin were then closed in layers and the animals allowed to recover on a heating pad until fully awake. For a double conditioning lesion, the sciatic nerve was completely transected with microscissors (Fine Science Tool, Foster City, CA) 3 days before the unilateral L4-L5 root crush and again, ~1 cm proximal to the site of the first transection, 7 days after DR crush. This sequence of a double conditioning lesion paradigm has been reported to enhance regeneration of DRG axons ascending in the dorsal columns after spinal cord injury (Neumann et al., 2005).

Production and microinjection of AAV2-GFP, LV-chABC and LV-GDNF. Recombinant self-complementary adeno-associated virus 2 (scAAV2) carrying eGFP was generated by helper virus-free system (Ayuso et al., 2010) as described previously (Liu et al., 2014). Replication deficient lentiviruses encoding either chABC (LV-chABC) or GDNF (LV-GDNF) used a pBOB lentiviral expression vector with CMV-enhanced chicken β-actin (CAG) promoter. The procedures to generate the viruses and their efficacy were described before: LV-chABC (Curinga et al., 2007; Jin et al., 2011; Han et al., 2017); LV-GDNF (Zhang et al., 2009a; Deng et al., 2013; Zhang et al., 2013; Kelamangalath et al., 2015; Han et al., 2017). AAV2-GFP was microinjected into lumbar DRGs using a micropipette pulled to a diameter of 0.05 mm and a nanoinjector (World Precision Instruments, Sarasota, FL). The viruses were injected at the time of DR crush. For each injection, the micropipette was introduced 0.5 mm into the DRG and a total volume of AAV (0.8 μl) containing $>2x10^{12}$ GC/ml injected over a 10 min period. The glass needle was left in place for 2 min after each injection. For LV-GDNF, five injections of 0.3μl lentivirus (a total of 2×10^{7} viral particles) were equally spaced rostrocaudally along the L4–L5 DREZ. Injections were made at a rate of 100 nl/min at a depth of 0.25mm from the spinal cord dorsal surface.

Tissue processing, selection and immunohistochemistry. Two or four weeks after DR crush, mice were sacrificed by an overdose of Euthasol and perfused transcardially with 0.9% saline followed by 4% paraformaldehyde (PFA) in 0.1M phosphate buffer (PBS, pH=7.4). The spinal cords with attached dorsal roots and DRGs were removed and examined in wholemounts to exclude those tissues with poor transduction of AAV2-GFP and/or spared axons. Properly lesioned and GFP+ tissues were first examined in wholemounts to assess DR regeneration across the DREZ. Tissues were then processed for analysis on cryostat sections. One or two representative tissues were processed for immunohistochemistry in spinal cord wholemounts. For analysis on cryostat sections, spinal cords were post-fixed in 4% PFA overnight at 4°C and cryoprotected in 30% sucrose for 1-2 days. The tissues were then embedded in M-1 Embedding Matrix (Thermo Fisher Scientific, Waltham, MA), transversely sectioned at 20 μm using a cryostat (Leica Microsystems, Germany), and mounted directly on slides (Superfrost Plus, Fisher Scientific, Pittsburgh, PA). For immunolabeling, sections were rinsed three times in PBS for 30 min followed by 10 min incubation with 0.1 M glycine in PBS, and 15 min incubation with 0.2% Triton X-100, 2% bovine serum albumin (BSA) in PBS (TBP). Sections were incubated with primary antibodies overnight at 4°C, washed three times for 30 min with 2% BSA in PBS and incubated with secondary antibodies for 1 h at room temperature. After three rinses with PBS, sections were mounted in Vectashield (Vector Laboratories, Burlingame, CA) and stored at -20°C until examination. For wholemount immunostaining of spinal cords, spinal cords with attached DRs were post-fixed in 4% PFA for 2 h at 4°C and the dura mater removed. The spinal cord was then rinsed three times with PBS for 30 min, incubated for 10 min in 0.1M glycine in 2% BSA/PBS, and permeabilized with pre-cooled methanol at -20°C for 10 min. After extensive rinsing in PBS, the spinal cord was incubated with primary antibody diluted in TBP at room temperature overnight, rinsed thoroughly in TBP the following day, and incubated with secondary antibodies for 2 h at room temperature. After rinsing in PBS, a thin slice of dorsal spinal cord (~2 mm thick) with attached DR stumps was cut with a microscissors and mounted on slides in Vectashield (Vector Laboratories, Burlingame, CA).

Antibodies. Primary antibodies were used at the following concentrations for immunohistochemistry: rabbit anti-NF200 (1:500, Sigma, St. Louis, MO, #N4142), IB4-biotin conjugate (1:200, Sigma, St. Louis, MO, #L2140), rabbit anti-CGRP (1:2,000, Peninsula Labs,

San Carlos, CA, #T4032), chicken anti-GFP (1:1,000, Avés Labs Inc., Davis, CA, #GFP-1020), rabbit anti-GFAP (1:500, Agilent, Santa Clara, CA, #N1506). Secondary antibodies used were Alexa Fluor 647-goat anti-rabbit IgG (1:400, Invitrogen, , Indianapolis, IN, #31573), Fluorescein (FITC)-conjugated goat anti-rabbit IgG (1:400, Millipore, Temecula, CA, AP307F), Alexa Fluor 568-conjugated goat anti-mouse IgG1 (1:400, Invitrogen, Indianapolis, IN, A21124), Alexa-Fluor 568-conjugated goat anti-rabbit (1:400, Invitrogen, Indianapolis, IN, #A11011), rhodamine (TRITC) streptavidin (1:400, Jackson ImmunoResearch Labs Inc., West Grove, PA, #016-020-084), or Alexa Fluor 488-donkey anti-chicken IgG (1:400, Jackson ImmunoResearch Labs Inc., West Grove, PA, #703-545-155). DAPI nucleic acid stain (1:1000, Thermo Fisher Scientific, Pittsburgh, PA, #D1306) for cell nuclei or Nissl substance stain (1:200, Thermo Fisher Scientific, Pittsburgh, PA, #N21482) for neuronal cells was used to counterstain prior to final wash steps in PBS.

Microscopy and image acquisition. An Olympus BX53 microscope equipped with Orca-R2 CCD camera (Hamamatsu, Japan) controlled by MetaMorph Image Analysis Software (Molecular Devices, San Jose, CA) was used to examine serial cryostat sections and dorsal wholemounts. Z stacked images were acquired using the Axio Imager (Zeiss, Germany) upright fluorescence microscope and AxioVision Imaging System (Zeiss, Germany) software or a SP8 confocal microscope (Leica Microsystems, Buffalo Grove, IL). All images were processed using Imaris (Bitplane, Windsor, CT) and Adobe Photoshop (Adobe Inc. San Jose, CA).

Analysis of regeneration across the DREZ. The location of the DREZ, where DR axons stop their regeneration at the entrance of spinal cord, was demarcated by GFAP immunostaining of astrocytes. The white dotted lines (e.g., Figure 1D, 1E) denote the location of the outer (peripheral) boundary of the DREZ, as defined by GFAP immunolabeling of astrocytic processes that extend peripherally (termed here ‘astrocyte:PNS border’ or ‘astrocytic border’). When GFAP was not immunolabeled, the astrocyte:PNS border was identified based on the greater abundance of cell nuclei in the PNS than CNS. For comparative evaluation of regeneration across the DREZ, we considered that DR axons penetrated into the CNS when they extended at least 100μm beyond the astrocyte:PNS border. For quantitative analysis, digital images were captured from 3-6 representative, non-adjacent sections taken from L4 and L5 segments of each

mouse (n=3-8 mice per cohort). A raw image was converted to a binary image using ImageJ with a threshold that appropriately separated GFP and background fluorescence. Lines were drawn at 100 μm before the border (in PNS territory), at the DREZ outer border, and at 100 μm intervals into CNS territory. The number of intersections of GFP+ axons at these distances was counted. The number of axons that crossed the outer border was normalized by the number of GFP+ axons counted at 100 μm before the border in the PNS, and then averaged by the number of evaluated sections and animals. This quantification resulted in the 'axon number index' that indicated the relative number and distance of axons that regenerated into the CNS in each group of mice.

Statistical analysis. All statistical analyses were performed using PRISM 8.0 (GraphPad, San Diego, CA.). Statistical analysis was by two-way repeated measures analysis of variance (ANOVA) with Tukey's multiple comparison tests. All data are presented as mean ± SD. Results were considered statistically significant if the p-value was < 0.05.

COMPETING INTERESTS

The authors declare no competing financial interests.

ACKNOWLEDGMENTS

We thank Drs. Alan Tessler, Matt Grove and Harun Noristiani for critical reading of the manuscript. We greatly thank Dr. Binhai Zheng for *Rtn4/Mag/Omg* triple and *Rtn4/Omg* double knockout mice, Dr. Jae Lee for MAG mutant mice, and Yingpeng Liu for technical assistance with LV-chABC and LV-GDNF.

FUNDINGS

This work was supported by NIH NINDS (NS079631) and Shriners Hospitals for Children (86600, 84050) to Y.-J.S.

REFERENCES

Andrews, M. R., Czvitkovich, S., Dassie, E., Vogelaar, C. F., Faissner, A., Blits, B., Gage, F. H., ffrench-Constant, C., and Fawcett, J. W. (2009). Alpha9 integrin promotes neurite outgrowth on tenascin-C and enhances sensory axon regeneration. *J Neurosci, 29*(17), 5546-5557. doi:29/17/5546 [pii]

10.1523/JNEUROSCI.0759-09.2009

Ayuso, E., Mingozzi, F., and Bosch, F. (2010). Production, purification and characterization of adeno-associated vectors. *Curr Gene Ther, 10*(6), 423-436.

Blesch, A., Lu, P., Tsukada, S., Alto, L. T., Roet, K., Coppola, G., Geschwind, D., and Tuszynski, M. H. (2012). Conditioning lesions before or after spinal cord injury recruit broad genetic mechanisms that sustain axonal regeneration: superiority to camp-mediated effects. *Exp Neurol, 235*(1), 162-173. doi:10.1016/j.expneurol.2011.12.037

Busch, S. A., Horn, K. P., Cuascut, F. X., Hawthorne, A. L., Bai, L., Miller, R. H., and Silver, J. (2010). Adult NG2+ cells are permissive to neurite outgrowth and stabilize sensory axons during macrophage-induced axonal dieback after spinal cord injury. *J Neurosci, 30*(1), 255-265. doi:10.1523/jneurosci.3705-09.2010

Cafferty, W. B., Bradbury, E. J., Lidierth, M., Jones, M., Duffy, P. J., Pezet, S., and McMahon, S. B. (2008). Chondroitinase ABC-mediated plasticity of spinal sensory function. *J Neurosci, 28*(46), 11998-12009. doi:10.1523/jneurosci.3877-08.2008

Cafferty, W. B., Yang, S. H., Duffy, P. J., Li, S., and Strittmatter, S. M. (2007). Functional axonal regeneration through astrocytic scar genetically modified to digest chondroitin sulfate proteoglycans. *J Neurosci, 27*(9), 2176-2185. doi:27/9/2176 [pii]

10.1523/JNEUROSCI.5176-06.2007

Carlstedt, T. (1985). Regenerating axons form nerve terminals at astrocytes. *Brain Res, 347*(1), 188-191. doi:0006-8993(85)90911-4 [pii]

Carlstedt, T. (2008). Root repair review: basic science background and clinical outcome. *Restor Neurol Neurosci, 26*(2-3), 225-241.

Cheah, M., Andrews, M. R., Chew, D. J., Moloney, E. B., Verhaagen, J., Fässler, R., and Fawcett, J. W. (2016). Expression of an Activated Integrin Promotes Long-Distance Sensory Axon Regeneration in the Spinal Cord. *J Neurosci, 36*(27), 7283-7297. doi:10.1523/jneurosci.0901-16.2016

Chong, M. S., Woolf, C. J., Haque, N. S. K., and Anderson, P. N. (1999). Axonal regeneration from injured dorsal roots into the spinal cord of adult rats. *Journal of Comparative Neurology, 410*(1), 42-54.

Collins, A., Ibrahim, A., Li, D., Liadi, M., and Li, Y. (2019). Reconstruction of the Damaged Dorsal Root Entry Zone by Transplantation of Olfactory Ensheathing Cells. *Cell Transplant, 28*(9-10), 1212-1219. doi:10.1177/0963689719855938

Curinga, G. M., Snow, D. M., Mashburn, C., Kohler, K., Thobaben, R., Caggiano, A. O., and Smith, G. M. (2007). Mammalian-produced chondroitinase AC mitigates axon inhibition by chondroitin sulfate proteoglycans. *J Neurochem, 102*(1), 275-288. doi:JNC4530 [pii]

10.1111/j.1471-4159.2007.04530.x

Deng, L. X., Deng, P., Ruan, Y., Xu, Z. C., Liu, N. K., Wen, X., Smith, G. M., and Xu, X. M. (2013). A novel growth-promoting pathway formed by GDNF-overexpressing Schwann cells promotes propriospinal axonal regeneration, synapse formation, and partial recovery of function after spinal cord injury. *J Neurosci, 33*(13), 5655-5667. doi:10.1523/jneurosci.2973-12.2013

DePaul, M. A., Lin, C. Y., Silver, J., and Lee, Y. S. (2017). Combinatory repair strategy to promote axon regeneration and functional recovery after chronic spinal cord injury. *Sci Rep, 7*(1), 9018. doi:10.1038/s41598-017-09432-6

Di Maio, A., Skuba, A., Himes, B. T., Bhagat, S. L., Hyun, J. K., Tessler, A., Bishop, D., and Son, Y. J. (2011). In Vivo Imaging of Dorsal Root Regeneration: Rapid Immobilization and Presynaptic Differentiation at the CNS/PNS Border. *J Neurosci, 31*(12), 4569-4582. doi:31/12/4569 [pii]

10.1523/JNEUROSCI.4638-10.2011

Dickendesher, T. L., Baldwin, K. T., Mironova, Y. A., Koriyama, Y., Raiker, S. J., Askew, K. L., Wood, A., Geoffroy, C. G., Zheng, B., Liepmann, C. D., Katagiri, Y., Benowitz, L. I., Geller, H. M., and Giger, R. J. (2012). NgR1 and NgR3 are receptors for chondroitin sulfate proteoglycans. *Nat Neurosci, 15*(5), 703-712. doi:10.1038/nn.3070

El-Brolosy, M. A., and Stainier, D. Y. R. (2017). Genetic compensation: A phenomenon in search of mechanisms. *PLoS Genet, 13*(7), e1006780. doi:10.1371/journal.pgen.1006780

Filous, A. R., Tran, A., Howell, C. J., Busch, S. A., Evans, T. A., Stallcup, W. B., Kang, S. H., Bergles, D. E., Lee, S. I., Levine, J. M., and Silver, J. (2014). Entrapment via synaptic-like connections between NG2 proteoglycan+ cells and dystrophic axons in the lesion plays a role in regeneration failure after spinal cord injury. *J Neurosci, 34*(49), 16369-16384. doi:10.1523/jneurosci.1309-14.2014

Fink, K. L., Strittmatter, S. M., and Cafferty, W. B. (2015). Comprehensive Corticospinal Labeling with mu-crystallin Transgene Reveals Axon Regeneration after Spinal Cord Trauma in ngr1-/- Mice. *J Neurosci, 35*(46), 15403-15418. doi:10.1523/jneurosci.3165-15.2015

Fischer, G., Kostic, S., Nakai, H., Park, F., Sapunar, D., Yu, H., and Hogan, Q. (2011). Direct injection into the dorsal root ganglion: technical, behavioral, and histological observations. *J Neurosci Methods, 199*(1), 43-55. doi:10.1016/j.jneumeth.2011.04.021

Golding, J. P., Bird, C., McMahon, S., and Cohen, J. (1999). Behaviour of DRG sensory neurites at the intact and injured adult rat dorsal root entry zone: postnatal neurites become

paralysed, whilst injury improves the growth of embryonic neurites. *Glia*, *26*(4), 309-323. doi:10.1002/(SICI)1098-1136(199906)26:4<309::AID-GLIA5>3.0.CO;2-0 [pii]

Golding, J. P., Shewan, D., Berry, M., and Cohen, J. (1996). An in vitro model of the rat dorsal root entry zone reveals developmental changes in the extent of sensory axon growth into the spinal cord. *Molecular and Cellular Neuroscience*, *7*(3), 191-203. doi:10.1006/mcne.1996.0015

Graham, J. B., and Muir, D. (2016). Chondroitinase C Selectively Degrades Chondroitin Sulfate Glycosaminoglycans that Inhibit Axonal Growth within the Endoneurium of Peripheral Nerve. *PLoS ONE*, *11*(12), e0167682. doi:10.1371/journal.pone.0167682

Griffin, J. M., and Bradke, F. (2020). Therapeutic repair for spinal cord injury: combinatory approaches to address a multifaceted problem. *EMBO Mol Med*, *12*(3), e11505. doi:10.15252/emmm.201911505

Guo, W. L., Qu, W. R., Zeng, L. N., Qi, Z. P., Huang, C., Zhu, Z., and Li, R. (2019). l-Theanine and NEP1-40 promote nerve regeneration and functional recovery after brachial plexus root avulsion. *Biochem Biophys Res Commun*, *508*(4), 1126-1132. doi:10.1016/j.bbrc.2018.11.124

Guseva, D., and Chelyshev, Y. (2006). The Plasticity of the DRG Neurons Belonging to Different Subpopulations After Dorsal Rhizotomy. *Cell Mol Neurobiol*, *26*(7-8), 1223-1232.

Han, S. B., Kim, H., Lee, H., Grove, M., Smith, G. M., and Son, Y. J. (2017). Postinjury Induction of Activated ErbB2 Selectively Hyperactivates Denervated Schwann Cells and Promotes Robust Dorsal Root Axon Regeneration. *J Neurosci*, *37*(45), 10955-10970. doi:10.1523/JNEUROSCI.0903-17.2017

Han, S. B., Kim, H., Skuba, A., Tessler, A., Ferguson, T., and Son, Y. J. (2012). Sensory Axon Regeneration: A Review from an in vivo Imaging Perspective. *Exp Neurobiol*, *21*(3), 83-93. doi:10.5607/en.2012.21.3.83

Harvey, P. A., Lee, D. H., Qian, F., Weinreb, P. H., and Frank, E. (2009). Blockade of Nogo receptor ligands promotes functional regeneration of sensory axons after dorsal root crush. *J Neurosci*, *29*(19), 6285-6295. doi:29/19/6285 [pii]

10.1523/JNEUROSCI.5885-08.2009

Hoeber, J., König, N., Trolle, C., Lekholm, E., Zhou, C., Pankratova, S., Åkesson, E., Fredriksson, R., Aldskogius, H., and Kozlova, E. N. (2017). A Combinatorial Approach to Induce Sensory Axon Regeneration into the Dorsal Root Avulsed Spinal Cord. *Stem Cells Dev*, *26*(14), 1065-1077. doi:10.1089/scd.2017.0019

Ito, S., Nagoshi, N., Tsuji, O., Shibata, S., Shinozaki, M., Kawabata, S., Kojima, K., Yasutake, K., Hirokawa, T., Matsumoto, M., Takei, K., Nakamura, M., and Okano, H. (2018).

LOTUS Inhibits Neuronal Apoptosis and Promotes Tract Regeneration in Contusive Spinal Cord Injury Model Mice. *eNeuro, 5*(5). doi:10.1523/eneuro.0303-18.2018

Iwakawa, M., Mizoi, K., Tessler, A., and Itoh, Y. (2001). Intraspinal implants of fibrin glue containing glial cell line-derived neurotrophic factor promote dorsal root regeneration into spinal cord. *Neurorehabil Neural Repair, 15*(3), 173-182.

Jacques, S. J., Ahmed, Z., Forbes, A., Douglas, M. R., Vigenswara, V., Berry, M., and Logan, A. (2012). AAV8(gfp) preferentially targets large diameter dorsal root ganglion neurones after both intra-dorsal root ganglion and intrathecal injection. *Mol Cell Neurosci, 49*(4), 464-474. doi:10.1016/j.mcn.2012.03.002

Jin, Y., Ketschek, A., Jiang, Z., Smith, G., and Fischer, I. (2011). Chondroitinase activity can be transduced by a lentiviral vector in vitro and in vivo. *J Neurosci Methods, 199*(2), 208-213. doi:10.1016/j.jneumeth.2011.05.007

Kaiser, R., Waldauf, P., Ullas, G., and Krajcová, A. (2020). Epidemiology, etiology, and types of severe adult brachial plexus injuries requiring surgical repair: systematic review and meta-analysis. *Neurosurg Rev, 43*(2), 443-452. doi:10.1007/s10143-018-1009-2

Kelamangalath, L., Tang, X., Bezik, K., Sterling, N., Son, Y. J., and Smith, G. M. (2015). Neurotrophin selectivity in organizing topographic regeneration of nociceptive afferents. *Exp Neurol, 271*, 262-278. doi:10.1016/j.expneurol.2015.06.007

Kubota, S., Sidikejiang, W., Kudo, M., Inoue, K. I., Umeda, T., Takada, M., and Seki, K. (2019). Optogenetic recruitment of spinal reflex pathways from large-diameter primary afferents in non-transgenic rats transduced with AAV9/Channelrhodopsin 2. *J Physiol, 597*(19), 5025-5040. doi:10.1113/jp278292

Kwon, M. J., Shin, H. Y., Cui, Y., Kim, H., Thi, A. H., Choi, J. Y., Kim, E. Y., Hwang, D. H., and Kim, B. G. (2015). CCL2 Mediates Neuron-Macrophage Interactions to Drive Proregenerative Macrophage Activation Following Preconditioning Injury. *J Neurosci, 35*(48), 15934-15947. doi:10.1523/jneurosci.1924-15.2015

Lang, B. T., Cregg, J. M., DePaul, M. A., Tran, A. P., Xu, K., Dyck, S. M., Madalena, K. M., Brown, B. P., Weng, Y. L., Li, S., Karimi-Abdolrezaee, S., Busch, S. A., Shen, Y., and Silver, J. (2015). Modulation of the proteoglycan receptor PTPσ promotes recovery after spinal cord injury. *Nature, 518*(7539), 404-408. doi:10.1038/nature13974

Lee, D. H., and Lee, J. K. (2013). Animal models of axon regeneration after spinal cord injury. *Neurosci Bull, 29*(4), 436-444. doi:10.1007/s12264-013-1365-4

Lee, J. K., Geoffroy, C. G., Chan, A. F., Tolentino, K. E., Crawford, M. J., Leal, M. A., Kang, B., and Zheng, B. H. (2010). Assessing Spinal Axon Regeneration and Sprouting in Nogo-, MAG-, and OMgp-Deficient Mice. *Neuron, 66*(5), 663-670. doi:10.1016/j.neuron.2010.05.002

Lemons, M. L., Sandy, J. D., Anderson, D. K., and Howland, D. R. (2003). Intact aggrecan and chondroitin sulfate-depleted aggrecan core glycoprotein inhibit axon growth in the adult rat spinal cord. *Exp Neurol, 184*(2), 981-990. doi:10.1016/s0014-4886(03)00383-2

Li, C., Tropak, M. B., Gerlai, R., Clapoff, S., Abramow-Newerly, W., Trapp, B., Peterson, A., and Roder, J. (1994). Myelination in the absence of myelin-associated glycoprotein. *Nature, 369*(6483), 747-750. doi:10.1038/369747a0

Li, C. L., Li, K. C., Wu, D., Chen, Y., Luo, H., Zhao, J. R., Wang, S. S., Sun, M. M., Lu, Y. J., Zhong, Y. Q., Hu, X. Y., Hou, R., Zhou, B. B., Bao, L., Xiao, H. S., and Zhang, X. (2016). Somatosensory neuron types identified by high-coverage single-cell RNA-sequencing and functional heterogeneity. *Cell Res, 26*(8), 967. doi:10.1038/cr.2016.90

Li, M., Shibata, A., Li, C., Braun, P. E., McKerracher, L., Roder, J., Kater, S. B., and David, S. (1996). Myelin-associated glycoprotein inhibits neurite/axon growth and causes growth cone collapse. *J Neurosci Res, 46*(4), 404-414. doi:10.1002/(SICI)1097-4547(19961115)46:4<404::AID-JNR2>3.0.CO;2-K [pii]

10.1002/(SICI)1097-4547(19961115)46:4<404::AID-JNR2>3.0.CO;2-K

Li, S., Xue, C., Yuan, Y., Zhang, R., Wang, Y., Wang, Y., Yu, B., Liu, J., Ding, F., Yang, Y., and Gu, X. (2015). The transcriptional landscape of dorsal root ganglia after sciatic nerve transection. *Sci Rep, 5*, 16888. doi:10.1038/srep16888

Li, Y., Carlstedt, T., Berthold, C. H., and Raisman, G. (2004). Interaction of transplanted olfactory-ensheathing cells and host astrocytic processes provides a bridge for axons to regenerate across the dorsal root entry zone. *Exp Neurol, 188*(2), 300-308. doi:10.1016/j.expneurol.2004.04.021

S0014488604001712 [pii]

Lin, C. L., Heron, P., Hamann, S. R., and Smith, G. M. (2014). Functional distinction between NGF-mediated plasticity and regeneration of nociceptive axons within the spinal cord. *Neuroscience, 272*, 76-87. doi:10.1016/j.neuroscience.2014.04.053

Lindholm, T., Risling, M., Carlstedt, T., Hammarberg, H., Wallquist, W., Cullheim, S., and Sköld, M. K. (2017). Expression of Semaphorins, Neuropilins, VEGF, and Tenascins in Rat and Human Primary Sensory Neurons after a Dorsal Root Injury. *Front Neurol, 8*, 49. doi:10.3389/fneur.2017.00049

Liu, S., Bohl, D., Blanchard, S., Bacci, J., Saïd, G., and Heard, J. M. (2009). Combination of microsurgery and gene therapy for spinal dorsal root injury repair. *Mol Ther, 17*(6), 992-1002. doi:10.1038/mt.2009.23

Liu, Y., Keefe, K., Tang, X., Lin, S., and Smith, G. M. (2014). Use of self-complementary adeno-associated virus serotype 2 as a tracer for labeling axons: implications for axon regeneration. *PLoS ONE, 9*(2), e87447. doi:10.1371/journal.pone.0087447

Liu, Y., Kelamangalath, L., Kim, H., Han, S. B., Tang, X., Zhai, J., Hong, J. W., Lin, S., Son, Y. J., and Smith, G. M. (2016). NT-3 promotes proprioceptive axon regeneration when combined with activation of the mTor intrinsic growth pathway but not with reduction of myelin extrinsic inhibitors. *Exp Neurol, 283*(Pt A), 73-84. doi:10.1016/j.expneurol.2016.05.021

Liuzzi, F. J., and Lasek, R. J. (1987). Astrocytes block axonal regeneration in mammals by activating the physiological stop pathway. *Science, 237*(4815), 642-645.

Mar, F. M., Simões, A. R., Rodrigo, I. S., and Sousa, M. M. (2016). Inhibitory Injury Signaling Represses Axon Regeneration After Dorsal Root Injury. *Mol Neurobiol, 53*(7), 4596-4605. doi:10.1007/s12035-015-9397-6

Mason, M. R. J., Ehlert, E. M. E., Eggers, R., Pool, C. W., Hermening, S., Huseinovic, A., Timmermans, E., Blits, B., and Verhaagen, J. (2010). Comparison of AAV Serotypes for Gene Delivery to Dorsal Root Ganglion Neurons. *Molecular Therapy, 18*(4), 715-724. doi:10.1038/mt.2010.19

Montagutelli, X. (2000). Effect of the genetic background on the phenotype of mouse mutations. *J Am Soc Nephrol, 11 Suppl 16*, S101-105.

Muir, E., De Winter, F., Verhaagen, J., and Fawcett, J. (2019). Recent advances in the therapeutic uses of chondroitinase ABC. *Exp Neurol, 321*, 113032. doi:10.1016/j.expneurol.2019.113032

Neumann, S., Skinner, K., and Basbaum, A. I. (2005). Sustaining intrinsic growth capacity of adult neurons promotes spinal cord regeneration. *Proc Natl Acad Sci U S A, 102*(46), 16848-16852. doi:10.1073/pnas.0508538102

Neumann, S., and Woolf, C. J. (1999). Regeneration of dorsal column fibers into and beyond the lesion site following adult spinal cord injury. *Neuron, 23*(1), 83-91. doi:S0896-6273(00)80755-2 [pii]

Nichols, E. L., and Smith, C. J. (2020). Functional Regeneration of the Sensory Root via Axonal Invasion. *Cell Rep, 30*(1), 9-17.e13. doi:10.1016/j.celrep.2019.12.008

Niu, J., Ding, L., Li, J. J., Kim, H., Liu, J., Li, H., Moberly, A., Badea, T. C., Duncan, I. D., Son, Y. J., Scherer, S. S., and Luo, W. (2013). Modality-based organization of ascending somatosensory axons in the direct dorsal column pathway. *J Neurosci, 33*(45), 17691-17709. doi:10.1523/JNEUROSCI.3429-13.2013

O'Donovan, K. J., Ma, K., Guo, H., Wang, C., Sun, F., Han, S. B., Kim, H., Wong, J. K., Charron, J., Zou, H., Son, Y. J., He, Z., and Zhong, J. (2014). B-RAF kinase drives developmental axon growth and promotes axon regeneration in the injured mature CNS. *J Exp Med, 211*(5), 801-814. doi:10.1084/jem.20131780

O'Shea, T. M., Burda, J. E., and Sofroniew, M. V. (2017). Cell biology of spinal cord injury and repair. *J Clin Invest, 127*(9), 3259-3270. doi:10.1172/jci90608

Ohtake, Y., Saito, A., and Li, S. (2018). Diverse functions of protein tyrosine phosphatase σ in the nervous and immune systems. *Exp Neurol, 302*, 196-204. doi:10.1016/j.expneurol.2018.01.014

Palmisano, I., Danzi, M. C., Hutson, T. H., Zhou, L., McLachlan, E., Serger, E., Shkura, K., Srivastava, P. K., Hervera, A., Neill, N. O., Liu, T., Dhrif, H., Wang, Z., Kubat, M., Wuchty, S., Merkenschlager, M., Levi, L., Elliott, E., Bixby, J. L., Lemmon, V. P., and Di Giovanni, S. (2019). Epigenomic signatures underpin the axonal regenerative ability of dorsal root ganglia sensory neurons. *Nat Neurosci, 22*(11), 1913-1924. doi:10.1038/s41593-019-0490-4

Peng, X., Zhou, Z., Hu, J., Fink, D. J., and Mata, M. (2010). Soluble Nogo receptor down-regulates expression of neuronal Nogo-A to enhance axonal regeneration. *J Biol Chem, 285*(4), 2783-2795. doi:10.1074/jbc.M109.046425

Quaglia, X., Beggah, A. T., Seidenbecher, C., and Zurn, A. D. (2008). Delayed priming promotes CNS regeneration post-rhizotomy in Neurocan and Brevican-deficient mice. *Brain, 131*(Pt 1), 240-249. doi:awm279 [pii]

10.1093/brain/awm279

Ramer, L. M., Richter, M. W., Roskams, A. J., Tetzlaff, W., and Ramer, M. S. (2004). Peripherally-derived olfactory ensheathing cells do not promote primary afferent regeneration following dorsal root injury. *Glia, 47*(2), 189-206. doi:10.1002/glia.20054

Ramer, M. S., Duraisingam, I., Priestley, J. V., and McMahon, S. B. (2001). Two-tiered inhibition of axon regeneration at the dorsal root entry zone. *The Journal of neuroscience : the official journal of the Society for Neuroscience, 21*(8), 2651-2660.

Ramer, M. S., Priestley, J. V., and McMahon, S. B. (2000). Functional regeneration of sensory axons into the adult spinal cord. *Nature, 403*(6767), 312-316. doi:10.1038/35002084

Romero, M. I., Rangappa, N., Garry, M. G., and Smith, G. M. (2001). Functional regeneration of chronically injured sensory afferents into adult spinal cord after neurotrophin gene therapy. *The Journal of neuroscience : the official journal of the Society for Neuroscience, 21*(21), 8408-8416.

Smith, G. M., Falone, A. E., and Frank, E. (2012). Sensory axon regeneration: rebuilding functional connections in the spinal cord. *Trends Neurosci, 35*(3), 156-163. doi:10.1016/j.tins.2011.10.006

Son, Y. J. (2015). Synapsing with NG2 cells (polydendrocytes), unappreciated barrier to axon regeneration? *Neural Regen Res, 10*(3), 346-348. doi:10.4103/1673-5374.153672

Steinmetz, M. P., Horn, K. P., Tom, V. J., Miller, J. H., Busch, S. A., Nair, D., Silver, D. J., and Silver, J. (2005). Chronic enhancement of the intrinsic growth capacity of sensory neurons combined with the degradation of inhibitory proteoglycans allows functional

regeneration of sensory axons through the dorsal root entry zone in the mammalian spinal cord. *J Neurosci, 25*(35), 8066-8076. doi:25/35/8066 [pii]

10.1523/JNEUROSCI.2111-05.2005

Stensaas, L. J., Partlow, L. M., Burgess, P. R., and Horch, K. W. (1987). Inhibition of regeneration: the ultrastructure of reactive astrocytes and abortive axon terminals in the transition zone of the dorsal root. *Prog Brain Res, 71*, 457-468. doi:10.1016/s0079-6123(08)61846-4

Steward, O., Popovich, P. G., Dietrich, W. D., and Kleitman, N. (2012). Replication and reproducibility in spinal cord injury research. *Exp Neurol, 233*(2), 597-605. doi:10.1016/j.expneurol.2011.06.017

Steward, O., Zheng, B., and Tessier-Lavigne, M. (2003). False resurrections: distinguishing regenerated from spared axons in the injured central nervous system. *J Comp Neurol, 459*(1), 1-8. doi:10.1002/cne.10593

Tan, C. L., Kwok, J. C., Patani, R., Ffrench-Constant, C., Chandran, S., and Fawcett, J. W. (2011). Integrin activation promotes axon growth on inhibitory chondroitin sulfate proteoglycans by enhancing integrin signaling. *J Neurosci, 31*(17), 6289-6295. doi:10.1523/jneurosci.0008-11.2011

Tedeschi, A., Omura, T., and Costigan, M. (2017). CNS repair and axon regeneration: Using genetic variation to determine mechanisms. *Exp Neurol, 287*(Pt 3), 409-422. doi:10.1016/j.expneurol.2016.05.004

Tessler, A., Himes, B. T., Houle, J., and Reier, P. J. (1988). Regeneration of adult dorsal root axons into transplants of embryonic spinal cord. *J Comp Neurol, 270*(4), 537-548. doi:10.1002/cne.902700407

Thiede-Stan, N. K., and Schwab, M. E. (2015). Attractive and repulsive factors act through multi-subunit receptor complexes to regulate nerve fiber growth. *J Cell Sci, 128*(14), 2403-2414. doi:10.1242/jcs.165555

Tom, V. J., Steinmetz, M. P., Miller, J. H., Doller, C. M., and Silver, J. (2004). Studies on the development and behavior of the dystrophic growth cone, the hallmark of regeneration failure, in an in vitro model of the glial scar and after spinal cord injury. *J Neurosci, 24*(29), 6531-6539. doi:10.1523/JNEUROSCI.0994-04.2004

24/29/6531 [pii]

Vargas, M. E., and Barres, B. A. (2007). Why is Wallerian degeneration in the CNS so slow? *Annu Rev Neurosci, 30*, 153-179. doi:10.1146/annurev.neuro.30.051606.094354

Wang, R., King, T., Ossipov, M. H., Rossomando, A. J., Vanderah, T. W., Harvey, P., Cariani, P., Frank, E., Sah, D. W., and Porreca, F. (2008). Persistent restoration of sensory function by immediate or delayed systemic artemin after dorsal root injury. *Nat Neurosci, 11*(4), 488-496. doi:nn2069 [pii]

10.1038/nn2069

Wang, X., Hasan, O., Arzeno, A., Benowitz, L. I., Cafferty, W. B., and Strittmatter, S. M. (2012). Axonal regeneration induced by blockade of glial inhibitors coupled with activation of intrinsic neuronal growth pathways. *Exp Neurol, 237*(1), 55-69. doi:10.1016/j.expneurol.2012.06.009

Wu, D., Klaw, M. C., Connors, T., Kholodilov, N., Burke, R. E., Côté, M. P., and Tom, V. J. (2017). Combining Constitutively Active Rheb Expression and Chondroitinase Promotes Functional Axonal Regeneration after Cervical Spinal Cord Injury. *Mol Ther, 25*(12), 2715-2726. doi:10.1016/j.ymthe.2017.08.011

Wu, D., Klaw, M. C., Kholodilov, N., Burke, R. E., Detloff, M. R., Côté, M. P., and Tom, V. J. (2016). Expressing Constitutively Active Rheb in Adult Dorsal Root Ganglion Neurons Enhances the Integration of Sensory Axons that Regenerate Across a Chondroitinase-Treated Dorsal Root Entry Zone Following Dorsal Root Crush. *Front Mol Neurosci, 9*, 49. doi:10.3389/fnmol.2016.00049

Yao, M., Sun, H., Yuan, Q., Li, N., Li, H., Tang, Y., Leung, G. K., and Wu, W. (2019). Targeting proteoglycan receptor PTPσ restores sensory function after spinal cord dorsal root injury by activation of Erks/CREB signaling pathway. *Neuropharmacology, 144*, 208-218. doi:10.1016/j.neuropharm.2018.10.035

Yu, H., Fischer, G., Ferhatovic, L., Fan, F., Light, A. R., Weihrauch, D., Sapunar, D., Nakai, H., Park, F., and Hogan, Q. H. (2013). Intraganglionic AAV6 results in efficient and long-term gene transfer to peripheral sensory nervous system in adult rats. *PLoS ONE, 8*(4), e61266. doi:10.1371/journal.pone.0061266

Zhang, C., Jin, Y., Ziemba, K. S., Fletcher, A. M., Ghosh, B., Truit, E., Yurek, D. M., and Smith, G. M. (2013). Long distance directional growth of dopaminergic axons along pathways of netrin-1 and GDNF. *Exp Neurol, 250*, 156-164. doi:10.1016/j.expneurol.2013.09.022

Zhang, L., Ma, Z., Smith, G. M., Wen, X., Pressman, Y., Wood, P. M., and Xu, X. M. (2009a). GDNF-enhanced axonal regeneration and myelination following spinal cord injury is mediated by primary effects on neurons. *Glia, 57*(11), 1178-1191. doi:10.1002/glia.20840

Zhang, L., Zheng, S., Wu, H., Wu, Y., Liu, S., Fan, M., and Zhang, J. (2009b). Identification of BLyS (B lymphocyte stimulator), a non-myelin-associated protein, as a functional ligand for Nogo-66 receptor. *J Neurosci, 29*(19), 6348-6352. doi:10.1523/jneurosci.5040-08.2009

Zhang, Y., Zhang, X., Wu, D., Verhaagen, J., Richardson, P. M., Yeh, J., and Bo, X. (2007). Lentiviral-mediated expression of polysialic acid in spinal cord and conditioning lesion promote regeneration of sensory axons into spinal cord. *Mol Ther, 15*(10), 1796-1804.

Zuo, J., Neubauer, D., Dyess, K., Ferguson, T. A., and Muir, D. (1998). Degradation of chondroitin sulfate proteoglycan enhances the neurite-promoting potential of spinal cord tissue. *Exp Neurol, 154*(2), 654-662. doi:10.1006/exnr.1998.6951

FIGURE LEGENDS

Figure 1. Intraganglionic AAV2-GFP labels proprioceptive and mechanoreceptive axons

(A) Schematic illustration of intraganglionic injection of scAAV2-eGFP and a representative DRG showing infected neurons expressing GFP at 2 weeks post-injection. **(B)** Mice expressing GFP in >70% Nissl-stained neurons were used in the present study. **(C)** DRG transverse sections showing GFP+ neurons (arrows) co-expressing neurofilament (NF), IB4, or CGRP. **(D)** Quantitative comparisons of AAV2-GFP infected neurons illustrating preferential labeling of large-diameter myelinated NF+ neurons, which mediate proprioception and mechanoreception. n>20 sections, 3 mice. **(E)** A transverse section showing GFP+ axons along the root and within the right side of the spinal cord, projecting into dorsal column, deeper laminae of the dorsal horn and into the ventral horn. An arrow denotes superficial laminae I-IIi lacking GFP fluorescence. **(E', E")** Enlarged views of the superficial dorsal horn, illustrating lack of GFP-fluorescence where CGRP+ nociceptive axons (magenta) innervate. DH, dorsal horn; DR, dorsal root; VH; ventral horn. Scale bars=50μm **(A, C, E', E")**, 200μm **(E)**.

Figure 2. Additional strategies for complete lesions and evaluation of DR regeneration

DR regeneration in WT mice assessed in wholemounts (**A-D**) and transverse sections (**E, F**) 2 weeks after L4 and L5 DR crush. **(A)** Schematic illustration of crushing roots prior to intraganglionic AAV2-GFP injections to avoid labeling of degenerating distal stump axons. **(B)** Wholemount view of completely crushed L4 and L5 DRs illustrating hundreds of GFP+ axons terminated at the entrance of spinal cord. **(B', B")** Enlarged views illustrating most axons terminated near the border. **(C-C")** Wholemount views of incompletely crushed DRs showing spared axons with long intraspinal projections. Spared axons are easily detectable in

wholemounts and commonly observed in the outermost dorsal rootlets (arrows). **(D)** Wholemount view of L4 DREZ illustrating GFP+ axons that crossed the astrocyte: PNS border (dotted line) and terminated nearby. The astrocytic border is identified by GFAP immunostaining of astrocytes (red). Yellow line denotes spinal cord midline recognized by the midline vein. **(E)** Four-color immunolabeling of transverse sections illustrating limited penetration of GFP+ or CGRP+ axons through the DREZ. White dotted lines approximate the peripheral boundary of the DREZ (astrocyte: PNS border) by locating peripherally projecting astrocytic processes (red) or by greater abundance of cell nuclei in the PNS (blue). Axons rarely extended >200μm beyond the border. Arrowheads denote frequently observed axons that grew along the growth-permissive dura. Arrow denotes occasionally observed subdural axons located several hundred microns past the border. **(F)** Quantitative analysis of DR regeneration on transverse sections (13 sections, 3 mice). ~90% GFP+ axons terminated within ~100μm of the border. Axons growing farther than 100μm are considered as having penetrated the DREZ. DH, dorsal horn; DR, dorsal root; S.C., spinal cord. Scale bars=200μm **(B-B", C-C", D, E)**.

Figure 2-source data 1

Source data for quantifying regeneration across the DREZ

This excel file contains raw data used for quantitative analysis shown in Figure 2F.

The following figure supplements are available for Figure 2.

Figure 2-figure supplement 1. Side-by-side comparison of different mouse groups in wholemounts and transverse sections

Representative wholemount and transverse sections of WT and *Rtn4/Mag/Omg* tKO groups with or without additional removal of CSPGs and/or nerve conditioning lesion. Arrows in wholemounts of tKO+GDNF and tKO+GDNF+ChABC groups denote intensely fluorescent areas due to abundant subdural GFP+ axons. WT, wild type; tKO, triple knockout; wpi, weeks postinjury; ChABC, chondroitinase ABC; CL, conditioning lesion; dCL, double conditioning lesion; GDNF, Glial cell line-derived neurotrophic factor. Scale bars=200μm

Figure 2-figure supplement 2. Validation of DAPI as a marker of the CNS: PNS border

Two sets of WT transverse sections at 2 wpi (**A-A"'**, **B-B"'**), co-labeled for laminin (**A, B**), DAPI (**A', B'**) and GFAP (**A"', B"'**), illustrating that DAPI reveals the astrocyte: PNS border because cell nuclei are much more densely accumulated in the PNS than CNS. The astrocyte: PNS border (dotted line) delineated by laminin, DAPI and GFAP overlaps closely. Arrowheads in **B** denote radicular arteries also labeled for laminin, which can obscure precise delineation of the boundary. Arrows in **B"** denote astrocytic processes that invaded the PNS after root injury but are readily distinguished from parental astrocytes in CNS territory. Small and large asterisks indicate enlarged views of **B-B"'**. Scale bars=200μm

Figure 3. Genetic deletion of Nogo/MAG/OMgp elicits little intraspinal regeneration

DR regeneration in *Rtn4/Mag/Omg* tKO mice assessed in wholemounts (**D**) or transverse sections (**F**) 2 weeks after L4 and L5 DR crush. **(A)** Identification of triple null mutants (red) lacking Nogo (A, B, C), MAG and OMgp. **(B)** Schematic illustration of the experimental procedures. **(C)** Wholemount view of a WT mouse. **(C', C")** Enlarged views of L4 and L5 DREZ in (**C**). Arrows denote axons extending longer processes past the DREZ. **(D)** Wholemount views of a tKO mouse illustrating termination of hundreds of GFP+ axons near the astrocyte: PNS border (dotted line), as in WT mice. The astrocyte:PNS border is identified by GFAP immunostaining of astrocytes (red). **(D', D")** Enlarged views of L4 and L5 DREZ in (**D**). Arrows denote axons extending longer processes past the DREZ, which were also frequently observed in WT mice. **(E)** Representative transverse sections of WT mice. **(F)** Representative transverse sections of *Rtn4/Mag/Omg* tKO mice illustrating little if any enhanced regeneration of GFP+ axons across the DREZ. Arrows denote axons that grew dorsally along the pia matter, as also observed in WT mice. **(G)** Quantitative comparisons illustrating no significant difference in WT and *Rtn4/Mag/Omg* tKO mice. 100μm, p=0.9738, df=162; 200μm, p=0.5046, df=162; 300μm, p=0.1454, df=162. Two-way repeated-measures ANOVA with Sidak's multiple comparisons test (WT: 13 sections, 3 mice; tKO: 16 sections, 5 mice). S.C., spinal cord; ns, not significant. Scale bars=200μm (**C-C", D-D", E-E", F-F"**).

Figure 3-source data 1

Source data for quantifying regeneration across the DREZ

This excel file contains raw data used for quantitative analysis shown in Figure 3G.

Figure 4. Additional CSPG removal slightly increases intraspinal regeneration in tKO mice

DR regeneration in ChABC-expressed *Rtn4/Mag/Omg* tKO mice assessed in wholemounts (**C**) and transverse sections (**E-E'**) 2 weeks after L4 and L5 DR crush. **(A)** Schematic illustration of the experimental procedures. LV-ChABC was injected into ipsilateral dorsal horn at multiple locations rostrocaudally along the L4-L5 DREZ. **(B)** Wholemount views of a WT mouse. **(C)** Wholemount views of a ChABC-expressed tKO showing hundreds of GFP+ axons in L4 and L5 roots terminated near the astrocyte: PNS border (dotted line), as in WT and tKO mice. The astrocyte: PNS border is identified by GFAP immunostaining of astrocytes (red). **(D)** Representative transverse sections of a WT mouse. **(E)** Representative transverse sections of a ChABC-expressed tKO illustrating effective degradation of CSPGs and modestly enhanced intraspinal regeneration. CS-56 immunoreactivity is very low in ipsilateral dorsal horn (asterisks), indicating effective removal of inhibitory GAG chains of CSPGs. Arrowheads denote Schwann cell-associated CS-56 immunoreactivity, which is markedly reduced but discernable in ChABC-expressed tKO. **(E')** Enlarged views showing a few GFP+ axons that penetrated the DREZ and are located at the top of the dorsal horn (arrows); such axons were not observed in WT or *Rtn4/Mag/Omg* tKO mice. **(F)** Quantitative comparisons illustrating modestly improved regeneration in ChABC-expressed *Rtn4/Mag/Omg* tKO mice: ~15% GFP+ penetrated the DREZ and remained within ~200μm of the border. ChABC-expressed tKO vs. WT: 100μm, **p=0.0022, df=186; 200μm, ***p=0.0003, df=186; 300μm, p=0.4818, df=186. ChABC-expressed tKO vs. tKO: 100μm, **p=0.0086, df=186; 200μm, **p=0.0099, df=186; 300μm, p=0.9262, df=186. Two-way repeated-measures ANOVA with Sidak's multiple comparisons test (WT: 13 sections, 3 mice; tKO: 16 sections, 5 mice; ChABC-tKO: 14 sections, 3 mice). S.C., spinal cord; ns, not significant. Scale bars=200μm (**B, C, D, E-E')**.

Figure 4-source data 1

Source data for quantifying regeneration across the DREZ

This excel file contains raw data used for quantitative analysis shown in Figure 4F.

Figure 5. Chronic regeneration failure at the DREZ lacking Nogo/MAG/OMgp and CSPGs

DR regeneration in WT (**A-D**), *Rtn4/Mag/Omg* tKO (**E-G**), and ChABC-expressed *Rtn4/Mag/Omg* tKO mice (**H-K**) analyzed 4 weeks after L4 and L5 DR crush. **(A)** Schematic illustration of the experimental procedures. **(B)** Wholemount view of L5 DREZ in a WT mouse showing no noticeably enhanced regeneration into the spinal cord. **(C, C')** Transverse sections showing no improved penetration of GFP+ (green) and CGRP+ axons (magenta) through the DREZ. **(D)** Quantitative comparisons of WT mice at 2wpi and 4wpi illustrating no significant difference. 100μm, p=0.5292, df=102. Two-way repeated-measured ANOVA with Sidak's multiple comparisons test (WT-2wpi: 13 sections, 3 mice; WT-4wpi: 14 sections, 4 mice). **(E)** Wholemount view of L4-L5 DREZ in a tKO showing no marked increase in intraspinal regeneration. **(F, F')** Transverse sections of a tKO mouse showing GFP+ (green) and CGRP+ axons (magenta) remaining at the DREZ at 4 wpi. **(G)** Quantitative comparisons of tKO mice at 2wpi and 4wpi illustrating no significant difference. 100μm, p=0.5067, df=168; 200μm, p>0.9999, df=168; 300μm, p>0.9999, df=168. Two-way repeated-measures ANOVA with Sidak's multiple comparisons test (tKO-2wpi: 16 sections, 5 mice; tKO-4wpi: 14 sections, 5 mice). **(H)** Wholemount view of L4-L5 DREZ in a ChABC-expressed tKO showing no noticeably enhanced intraspinal regeneration. **(I. I')** Transverse sections of a ChABC-expressed tKO showing GFP+ (green) and CGRP+ axons (magenta) remaining at the DREZ at 4wpi. **(J)** Quantitative comparisons of ChABC-expressed tKO mice at 2wpi and 4wpi illustrating no significant increase in GFP+ axons that penetrated the DREZ. 100μm, p=0.0027, df=60; 200μm, p=0.936, df=60; 300μm, p>0.9999, df=60. Two-way repeated-measures ANOVA with Sidak's multiple comparisons test (ChABC-tKO-2wpi: 14 sections, 3 mice; ChABC-tKO-4wpi: 12 sections, 3 mice). **(K)** Quantitative comparisons of WT, tKO and ChABC-expressed tKO at 4wpi showing no significant difference in GFP+ axons crossing the DREZ. ChABC-expressed tKO vs. WT: 100μm, ***p=0.0001, df=144; 200μm, p=0.668, df=144; 300μm, p=0.7582, df=144). Two-way repeated-measures ANOVA with Sidak's multiple comparisons test. Scale bars=200μm (**B, C-C', E-F', H-I'**).

Figure 5-source data 1

Source data for quantifying regeneration across the DREZ

This excel file contains raw data used for quantitative analysis shown in Figure 4D, 4G, 4J, 4K.

Figure 6. Nerve conditioning lesion does not promote regeneration across the DREZ in tKO mice

(A) Schematic illustration of the experimental procedures. *Rtn4/Mag/Omg* tKO mice received a nerve conditioning lesion 10 days before L4 and L5 DR crush and were assessed at 2 wpi. **(B)** Wholemount view of a WT mouse. **(C)** Wholemount view of a conditioned tKO showing hundreds of GFP+ axons terminated near the astrocyte: PNS border (dotted line), as in WT and tKO mice. **(D)** Transverse sections of a WT mouse. **(E, E')** Transverse sections of a conditioned tKO illustrating little if any enhanced regeneration of GFP+ (green) or CGRP+ axons (magenta) across the DREZ. An arrow denotes occasionally observed GFP+ axons that reached dorsolateral grey matter. **(F)** Quantitative comparisons illustrating no significant difference in WT, tKO and conditioned tKO mice. tKO vs. conditioned tKO: 100μm, ****$p < 0.0001$, df=220; 200μm, $p = 0.9991$, df=220; 300μm, $p > 0.9999$, df=220. Two-way repeated-measures ANOVA with Sidak's multiple comparisons test (WT: 13 sections, 3 mice; tKO: 16 sections, 5 mice; conditioned-tKO: 11 sections, 3 mice). ns, not significant. Scale bars=200μm (**B, C, D, E, E')**.

Figure 6-source data 1

Source data for quantifying regeneration across the DREZ

This excel file contains raw data used for quantitative analysis shown in Figure 6F.

The following figure supplements are available for Figure 6.

Figure 6-figure supplement 1. Double conditioning lesion modestly enhances regeneration across the DREZ in WT mice

(A) Schematic illustration of the experimental procedures. WT mice received two conditioning lesions (WT+dCL); the ipsilateral sciatic nerve was transected 3 days before and 7 days after L4 and L5 DR crush. Mice were assessed at 2 wpi. Wholemount and transverse section views of double lesioned WT mice **(D, G, H)** are presented side-by-side with those of WT **(B, E)**, single lesioned tKO **(C, F)** and GDNF-expressed WT mice **(I)**. **(B)** Wholemount view of a WT that received no conditioning lesion. **(C)** Wholemount view of a *Rtn4/Mag/Omg* tKO mouse that received a single nerve crush conditioning lesion. **(D)** Wholemount view of a WT mouse that received two conditioning lesions showing hundreds of GFP+ axons terminated near the astrocyte: PNS border (dotted line), as in WT and single lesioned tKO mice. **(E)** Transverse

sections of a WT that received no conditioning lesion. **(F)** Transverse sections of a *Rtn4/Mag/Omg* tKO mouse that received a single conditioning lesion. **(G, H)** Transverse sections of a WT mouse that received two conditioning lesions. Arrows indicate occasional GFP+ axons that enter dorsal grey matter. **(I)** Transverse sections of a GDNF-expressed WT showing numerous GFP+ axons that enter grey matter. See also Figure 8. **(J)** Quantitative comparisons illustrating modest regeneration of double conditioned DR axons through the DREZ: ~10% GFP+ axons extended ~100μm past the DREZ. 100μm, ****p<0.0001, df=426 (WT vs WT+dCL, WT+dCL vs WT+GDNF), p=0.8369, df=426 (WT+dCL vs tKO+CL); 200μm, *p=0.0239, df=426 (WT vs WT+dCL), ****p<0.0001, df=426, p=0.2695, df=426 (WT+dCL vs tKO+CL); 300 μm, p=0.6437; df=426 (WT vs WT+dCL), ****p<0.0001, df=426 (WT+dCL vs WT+GDNF); p=0.7119, df=426 (WT+dCL vs tKO+CL); 400μm, **p=0.0030, df=426 (WT+dCL vs WT+GDNF). Two-way repeated-measures ANOVA with Sidak's multiple comparisons test (WT: 13 sections, 3 mice; tKO+CL: 11 sections, 3 mice; WT+dCL: 37 sections, 4 mice; WT+GDNF: 15 sections, 3 mice). Scale bars=200μm **(B-I)**.

Figure 6-figure supplement 1-source data 1

Source data for quantifying regeneration across the DREZ

This excel file contains raw data used for quantitative analysis shown in Figure 6-figure supplement 1J.

Figure 7. Additional CSPG removal minimally enhances regeneration of conditioning lesioned axons in tKO mice

(A) Schematic illustration of the experimental procedures. LV-ChABC was injected into *Rtn4/Mag/Omg* tKO mice that received a conditioning lesion 10 days before L4 and L5 DR crush. **(B)** Wholemount view of a WT mouse. **(C)** Wholemount view of a ChABC/conditioned tKO showing hundreds of GFP+ axons that remain near the border (dotted line). **(D)** Transverse sections of a WT mouse. **(E-E')** Transverse sections of a ChABC/conditioned tKO illustrating effective CSPG degradation confirmed by the lack of CS-56 immunoreactivity (asterisks) and little if any intraspinal regeneration of GFP+ axons. **(F-F')** Additional transverse sections of a ChABC/conditioned tKO illustrating limited intraspinal regeneration of GFP+ or CGRP+ axons (magenta). Arrows denote occasionally observed GFP+ axons that enter dorsal grey matter. **(G)**

Quantitative comparisons illustrating no significant difference in ChABC/conditioned tKO and conditioned tKO mice. 100μm, p=0.7629, df=114; 200μm, p=0. 2671, df=114. Two-way repeated-measures ANOVA with Sidak's multiple comparisons test (conditioned tKO: 11 sections, 3 mice; ChABC/conditioned tKO: 10 sections, 4 mice). **(H)** Quantitative summary illustrating minimal intraspinal regeneration of even conditioned axons after concurrent removal of myelin inhibitors and CSPGs; Only ~10% GFP+ axons extended ~100um past the DREZ. 100μm, *p=0.0488, df=300 (WT vs ChABC expressed tKO), ****p<0.0001, df=300 (WT vs conditioned tKO, WT vs ChABC/conditioned tKO); 200μm, *p=0.014, df = 300 (WT vs ChABC expressed tKO, **p=0.0024, df = 300 (WT vs ChABC/conditioned tKO); 300 μm, p>0.9999; df = 300. Two-way repeated-measures ANOVA with Sidak's multiple comparisons test. Scale bars=200μm (**B, C, D, E-E', F-F')**.

Figure 7-source data 1

Source data for quantifying regeneration across the DREZ

This excel file contains raw data used for quantitative analysis shown in Figure 7G and 7H.

Figure 8. Nogo/MAG/OMgp removal markedly enhances regeneration of GDNF-stimulated DR axons

GDNF-induced intraspinal regeneration analyzed in WT (**A-D**) and *Rtn4/Mag/Omg* tKO mice (**E-H**) 2 weeks after L4 and L5 DR crush. **(A)** Schematic illustration showing intraspinal injections of LV-GDNF at the time of root crush and AAV2-GFP injections in WT mice. **(B)** Wholemount view of a GDNF-expressed WT illustrating hundreds of GFP+ axons largely remaining near the border. **(C-C')** Transverse sections of a GDNF-expressed WT showing a number of GFP+ (green) or CGRP+ axons (magenta) that cross the DREZ and extend further into the dorsal funiculus and grey matter. **(D)** Quantitative comparisons illustrating significantly enhanced penetration of GFP+ axons across the DREZ. 100μm, 200μm and 300μm, ****p<0.0001, df=156; 400μm, p=0.2446, df=156. Two-way repeated-measures ANOVA with Sidak's multiple comparisons test (WT: 13 sections, 3 mice; GDNF-expressed WT: 15 sections, 3 mice). **(E)** Schematic illustration of the experimental procedures in *Rtn4/Mag/Omg* tKO mice. **(F)** Wholemount view of a GDNF-expressed tKO mouse revealing intensely fluorescent area of the L4 and L5 DREZ (arrows), likely due to densely accumulated subdural GFP+ axons. **(G-G')**

Transverse sections of a GDNF-expressed tKO mouse displaying numerous GFP+ axons regenerating deep into dorsal horn. Asterisks denote CGRP immunoreactivity in deep dorsal laminae (magenta), presumably indicating enhanced regeneration of CGRP+ axons in GDNF-expressed tKO, as compared to that in GDNF-expressed WT. **(H)** Quantitative comparisons illustrating markedly greater intraspinal growth of GFAP-labeled axons in GDNF-expressed tKO than in GDNF-expressed WT mice. 100μm and 200μm, ****p<0.0001, df=174; 300μm, *p=0.028, df=174; 400μm, p=0.9975, df=174. Two-way repeated-measures ANOVA with Sidak's multiple comparisons test (GDNF-expressed WT: 15 sections, 3 mice; GDNF-expressed tKO: 16 sections, 5 mice). ns, not significant. Scale bars=200μm (**B, C, C', F, G, G')**.

Figure 8-source data 1

Source data for quantifying regeneration across the DREZ

This excel file contains raw data used for quantitative analysis shown in Figure 8D and 8H.

Figure 9. CSPG removal further enhances regeneration of GDNF-stimulated axons in tKO mice

(A) Schematic illustration of the experimental procedures. LV-ChABC and LV-GDNF were injected into dorsal horn along the L4-L5 DREZ in *Rtn4/Mag/Omg* tKO mice. **(B)** Wholemount view of a GDNF-expressed WT mouse. **(C)** Wholemount view of a ChABC/GDNF-expressed tKO showing broader areas of the DREZ and the CNS with densely accumulated GFP+ axons (arrows). Arrowheads denote numerous axons extending rostrocaudally close to the midline. **(D)** Transverse sections of a GDNF-expressed WT mouse. **(E-E')** Transverse sections of a ChABC/GDNF-expressed tKO showing effective degradation of CSPGs confirmed by CS-56 immunoreactivity and many GFP+ axons densely filling broad and deep areas of the dorsal horn. **(F)** Transverse sections of a ChABC/GDNF-expressed tKO showing enhanced intraspinal regeneration of GFP+ axons and CGRP+ axons (magenta). CGRP+ immunoreactivity is bright, dense, and remarkably restricted to the superficial laminae. **(G)** Quantitative comparisons illustrating significantly more GFP+ axons in deeper portions of the dorsal horn in ChABC/GDNF-expressed tKO. 100μm, p=0.5389, df=210; 200μm, p=0.9891, df=210; 300μm, p=0.2358, df=210; 400μm, p=0.0074, df=210; 500μm, p=0.5805, df=210. Two-way repeated-measures ANOVA with Sidak's multiple comparisons test (ChABC/GDNF-expressed tKO: 19

sections, 8 mice; GDNF-expressed tKO: 16 sections, 5 mice). ns, not significant. Scale bars=200μm (**B, C, D, E-E', F**).

Figure 9-source data 1

Source data for quantifying regeneration across the DREZ

This excel file contains raw data used for quantitative analysis shown in Figure 9G.

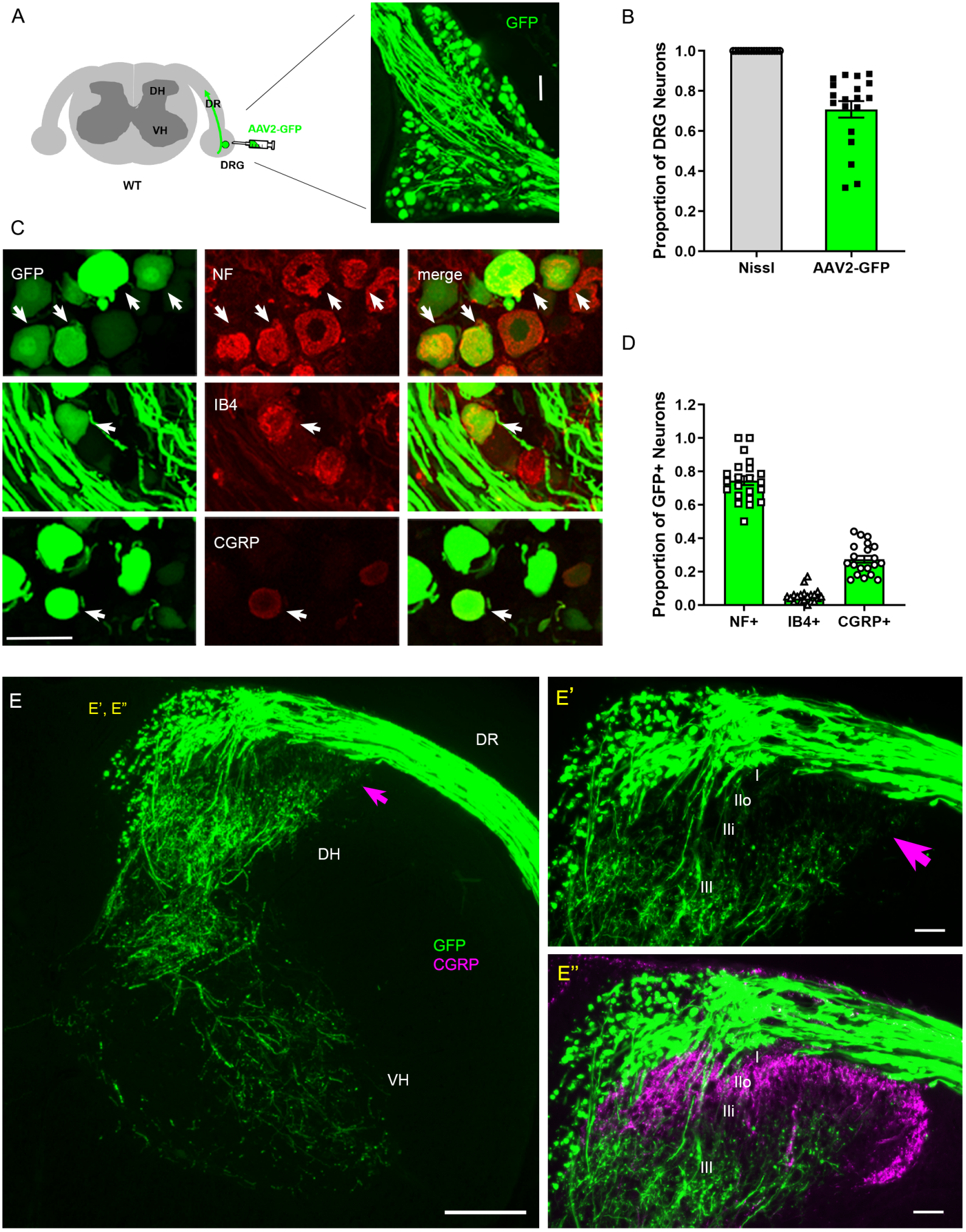
A
DH
VH
DR
AAV2-GFP
DRG
WT
GFP
I
B
Proportion of DRG Neurons
1.0
0.8
0.6
0.4
0.2
0.0
Nissl
AAV2-GFP
C
GFP
NF
merge
IB4
CGRP
D
Proportion of GFP+ Neurons
1.2
1.0
0.8
0.6
0.4
0.2
0.0
NF+
IB4+
CGRP+
E
E', E"
DR
DH
GFP
CGRP
VH
E'
I
IIo
IIi
III
E"
I
IIo
IIi
III

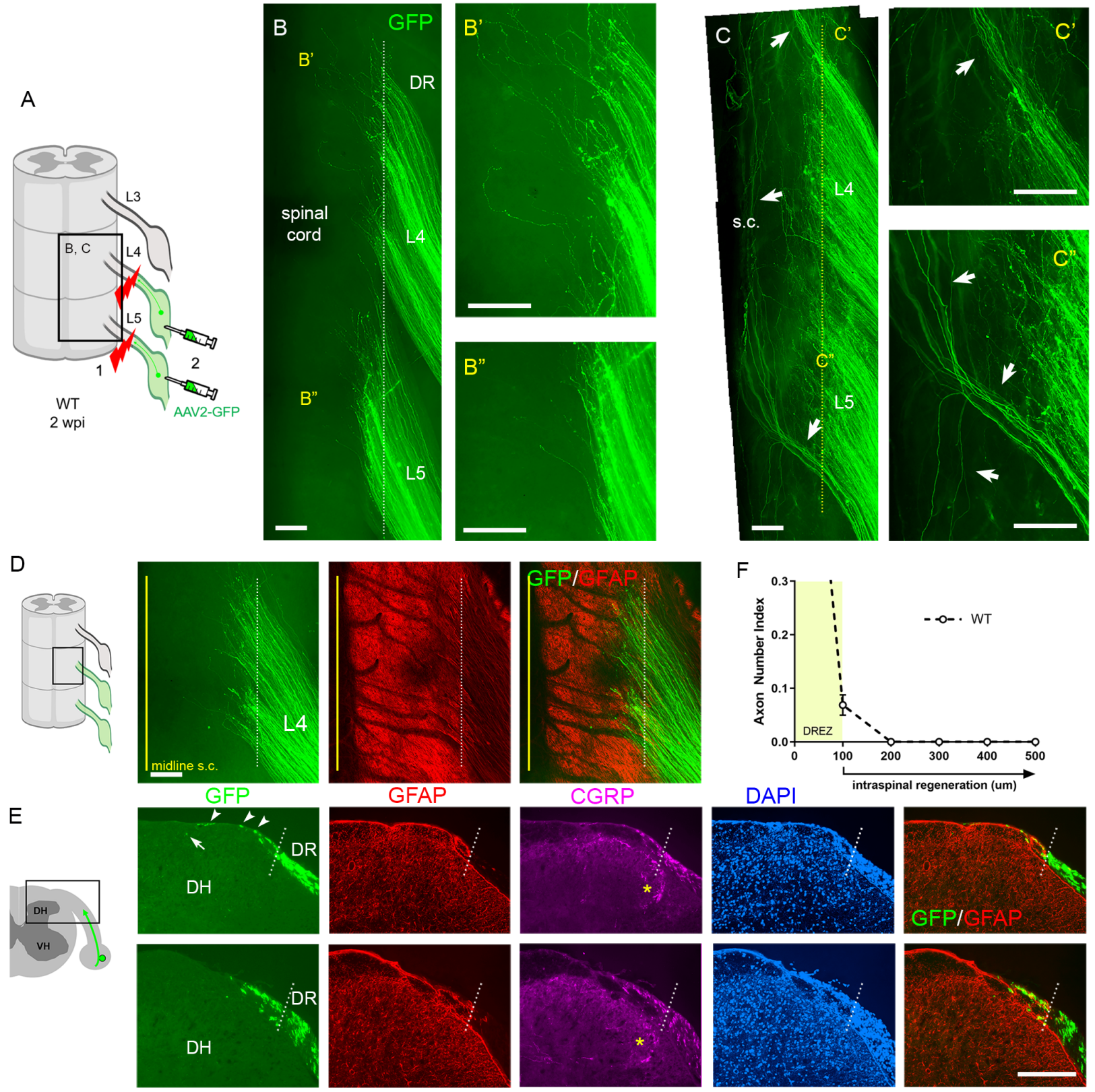
A
L3
L4
L5
B, C
1
2
WT
2 wpi
AAV2-GFP
B
GFP
B'
DR
spinal
cord
L4
B"
L5
B'
B"
C
C'
s.c.
L4
C"
L5
C'
C"
D
L4
midline s.c.
GFP/GFAP
E
GFP
GFAP
CGRP
DAPI
DR
DH
VH
GFP/GFAP
F
Axon Number Index
0.3
0.2
0.1
0.0
WT
DREZ
0
100
200
300
400
500
intraspinal regeneration (um)

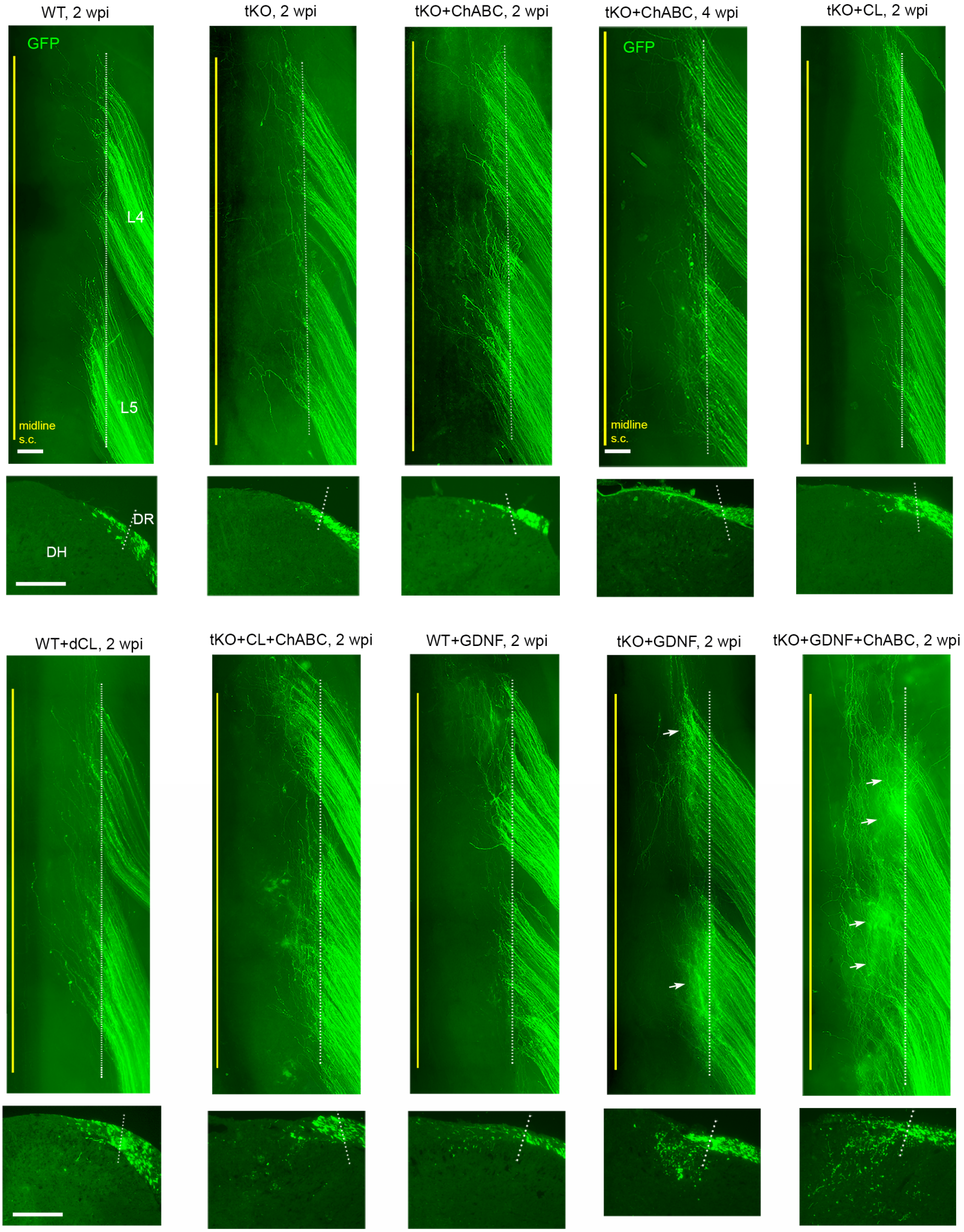
WT, 2 wpi
tKO, 2 wpi
tKO+ChABC, 2 wpi
tKO+ChABC, 4 wpi
tKO+CL, 2 wpi
GFP
L4
L5
midline
s.c.
DR
DH
WT+dCL, 2 wpi
tKO+CL+ChABC, 2 wpi
WT+GDNF, 2 wpi
tKO+GDNF, 2 wpi
tKO+GDNF+ChABC, 2 wpi

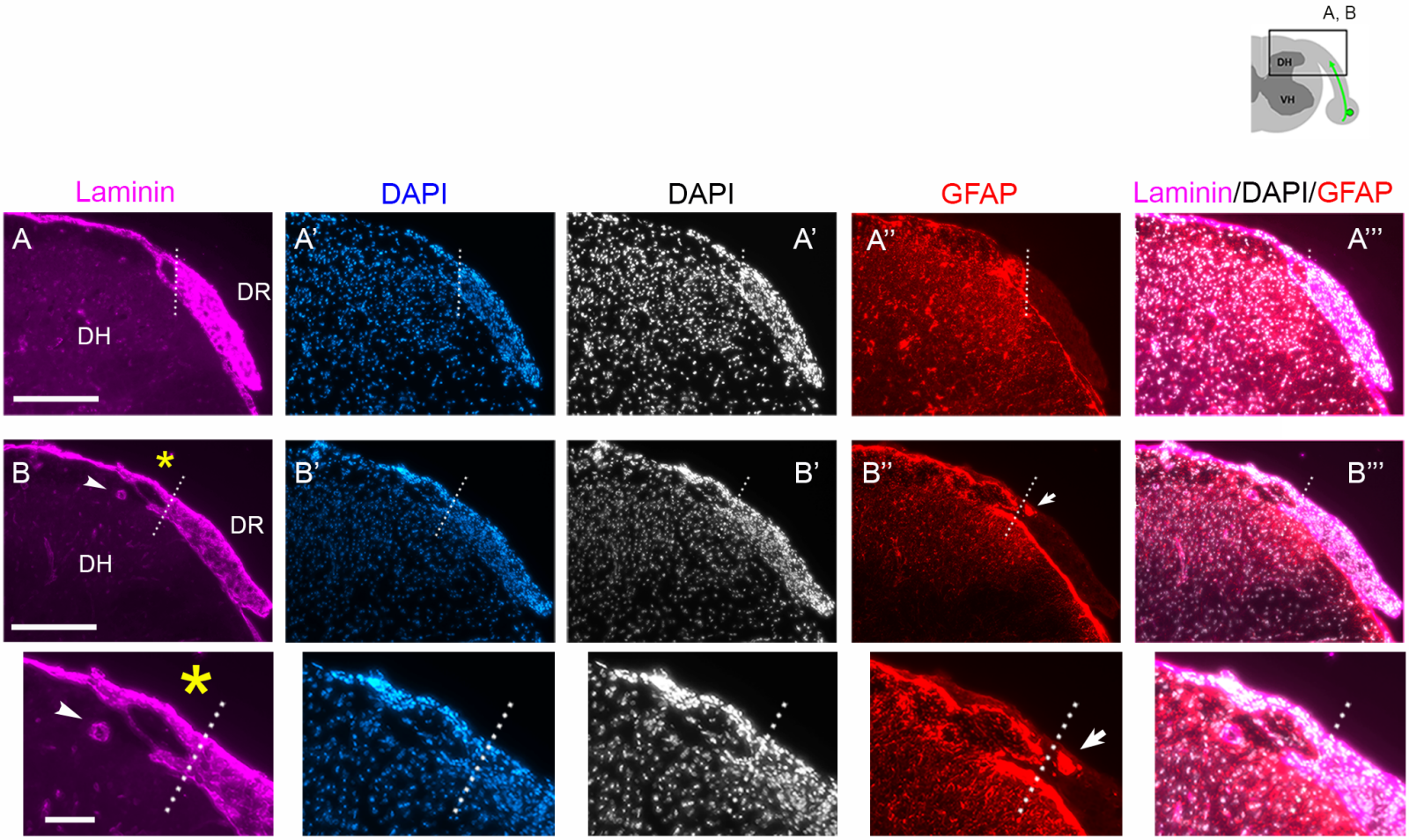
A, B
DH
VH
Laminin
DAPI
DAPI
GFAP
Laminin/DAPI/GFAP
A
A'
A'
A''
A'''
DR
DH
B
B'
B'
B''
B'''
DR
DH

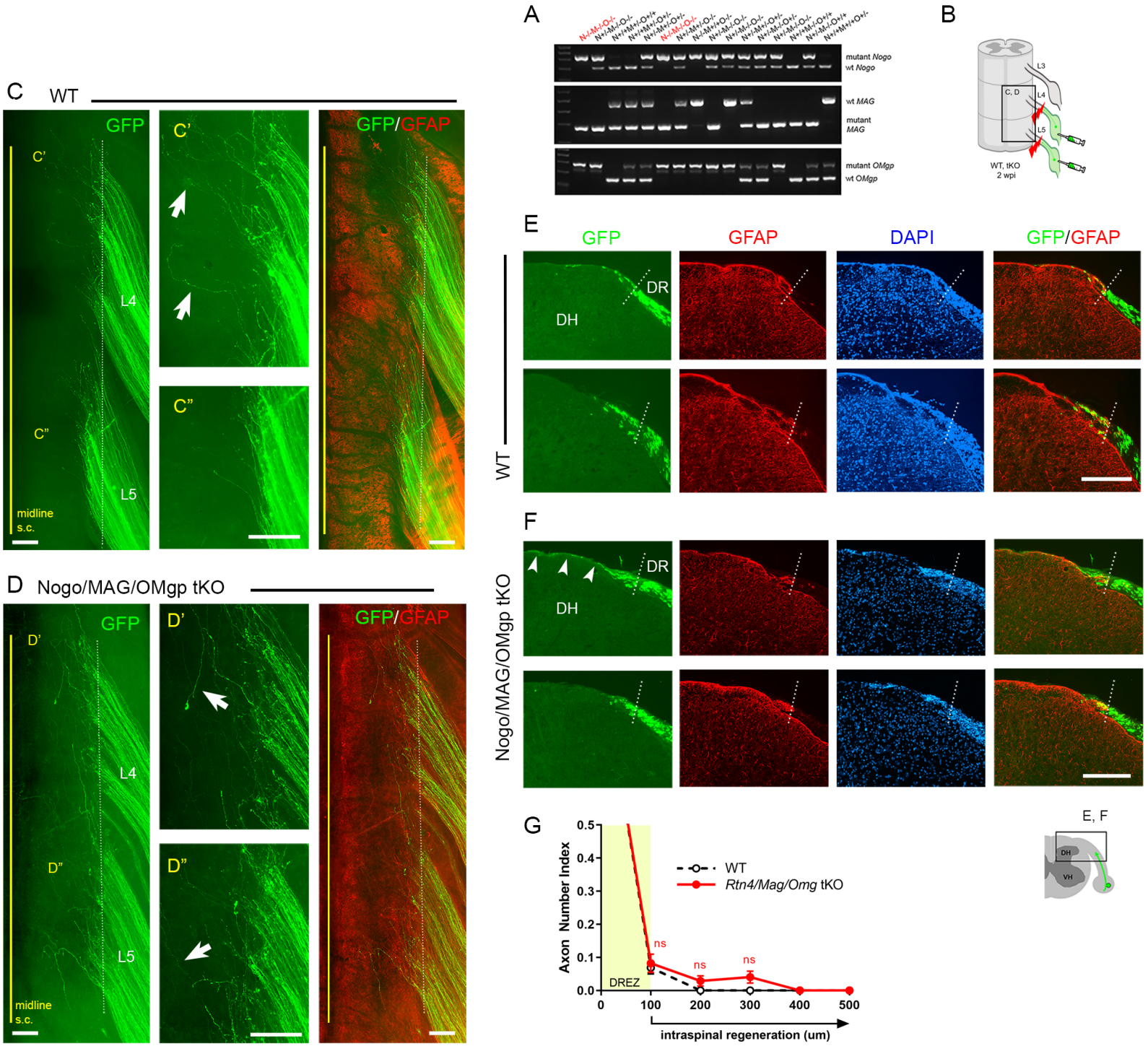
A
mutant Nogo
wt Nogo
wt MAG
mutant MAG
mutant OMgp
wt OMgp
B
L3
L4
L5
C, D
WT, tKO
2 wpi
C WT
GFP
C'
C"
L4
L5
midline
s.c.
GFP/GFAP
D Nogo/MAG/OMgp tKO
D'
D"
E
GFP
GFAP
DAPI
GFP/GFAP
DR
DH
WT
F
Nogo/MAG/OMgp tKO
G
Axon Number Index
WT
Rtn4/Mag/Omg tKO
ns
DREZ
intraspinal regeneration (um)
E, F
DH
VH

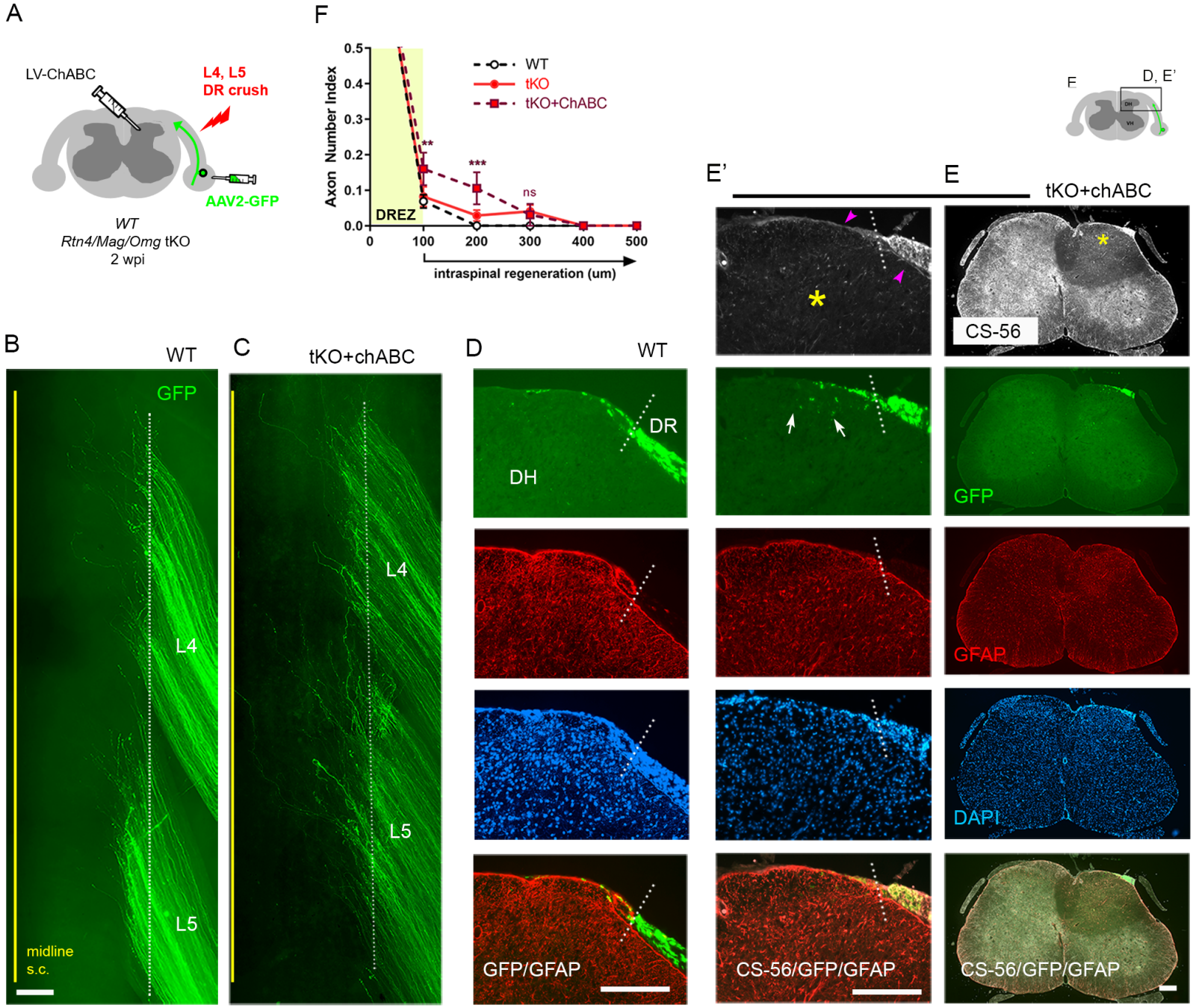
A
LV-ChABC
L4, L5
DR crush
AAV2-GFP
WT
Rtn4/Mag/Omg tKO
2 wpi
F
Axon Number Index
0.5
0.4
0.3
0.2
0.1
0.0
DREZ
WT
tKO
tKO+ChABC
**
***
ns
0
100
200
300
400
500
intraspinal regeneration (um)
E
D, E'
DH
VH
E'
E
tKO+chABC
CS-56
GFP
GFAP
DAPI
GFP/GFAP
CS-56/GFP/GFAP
CS-56/GFP/GFAP
B
WT
GFP
L4
L5
midline
s.c.
C
tKO+chABC
L4
L5
D
WT
DR
DH

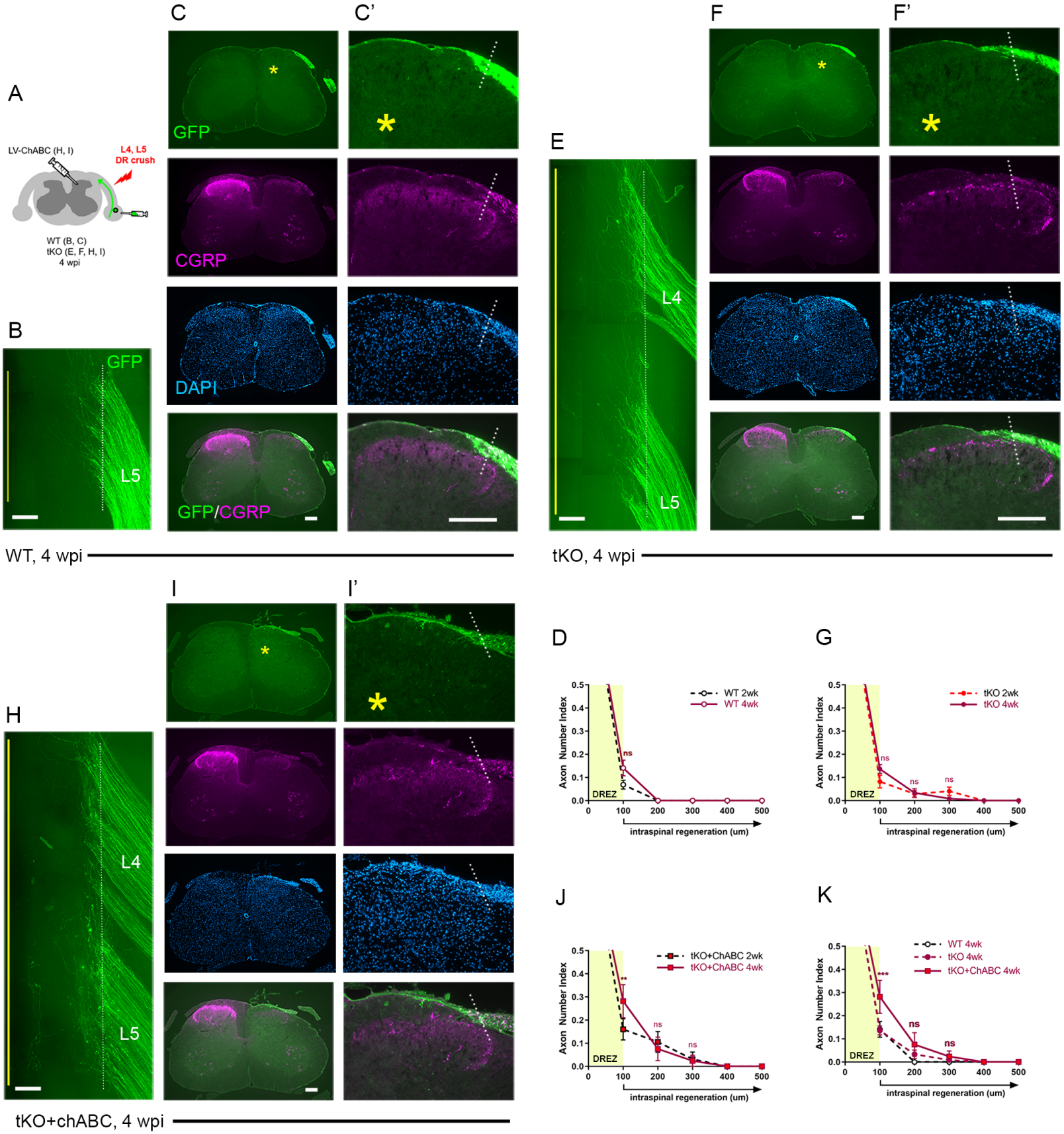
A
LV-ChABC (H, I)
L4, L5
DR crush
WT (B, C)
tKO (E, F, H, I)
4 wpi
B
GFP
L5
C
C'
GFP
CGRP
DAPI
GFP/CGRP
WT, 4 wpi
E
L4
L5
F
F'
tKO, 4 wpi
H
L4
L5
I
I'
tKO+chABC, 4 wpi
D
WT 2wk
WT 4wk
Axon Number Index
DREZ
intraspinal regeneration (um)
G
tKO 2wk
tKO 4wk
J
tKO+ChABC 2wk
tKO+ChABC 4wk
K
WT 4wk
tKO 4wk
tKO+ChABC 4wk
ns
**
***

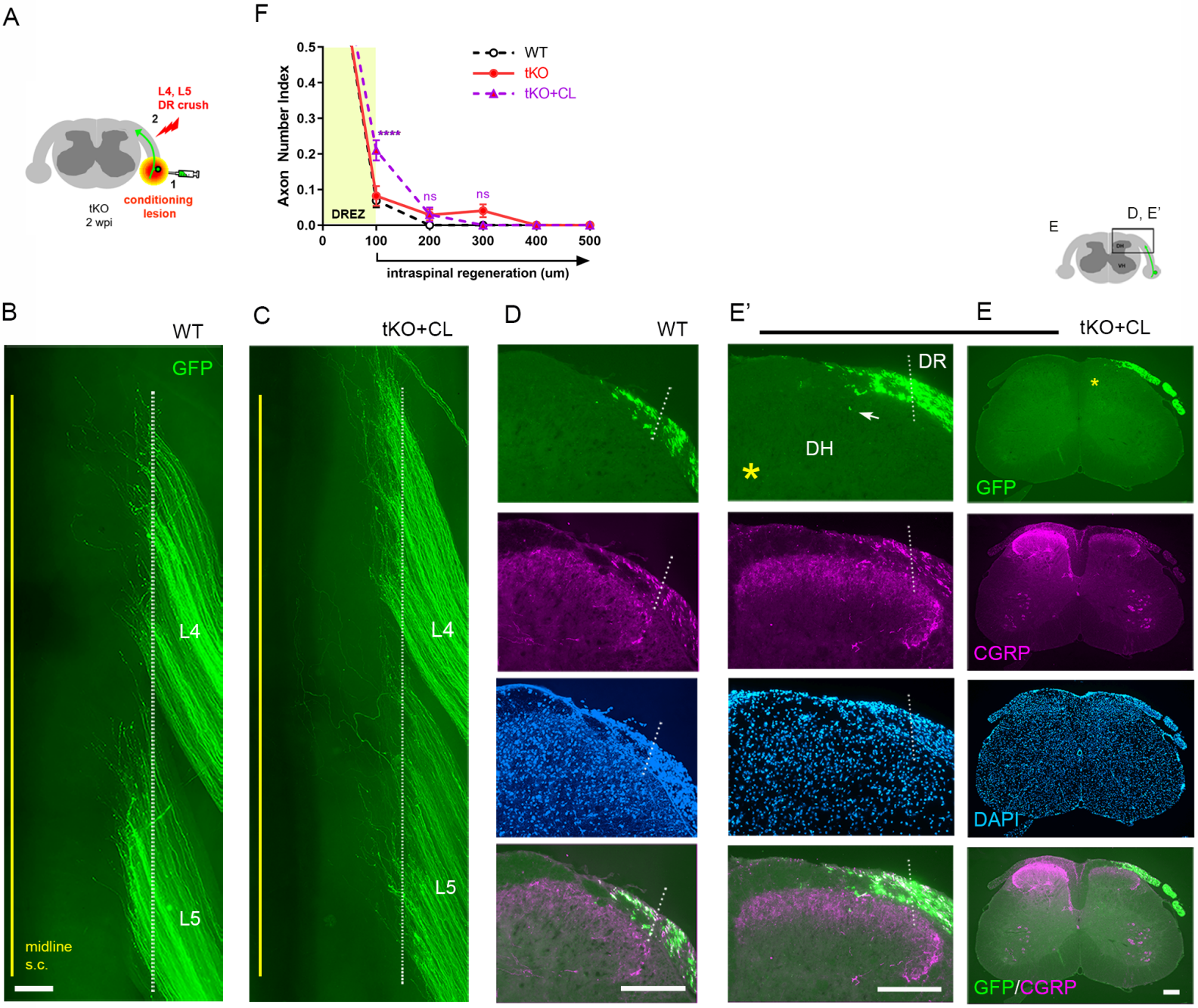
A
L4, L5
DR crush
2
1
conditioning
lesion
tKO
2 wpi
F
WT
tKO
tKO+CL
Axon Number Index
0.5
0.4
0.3
0.2
0.1
0.0
DREZ
****
ns
ns
0
100
200
300
400
500
intraspinal regeneration (um)
E
D, E'
B
WT
GFP
L4
L5
midline
s.c.
C
tKO+CL
L4
L5
D
WT
E'
E
tKO+CL
DR
DH
*
GFP
CGRP
DAPI
GFP/CGRP

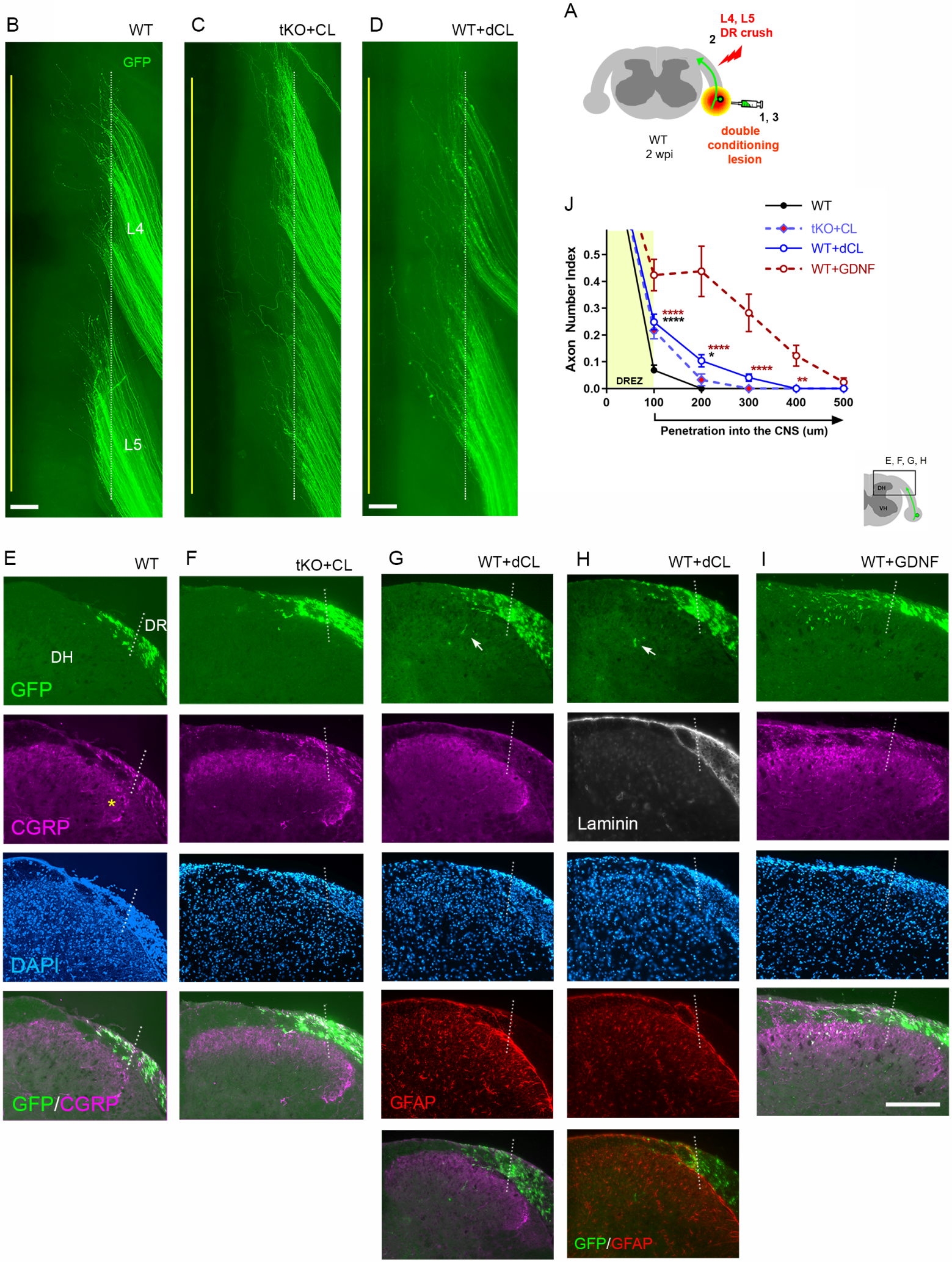
B
WT
GFP
L4
L5
C
tKO+CL
D
WT+dCL
A
L4, L5
DR crush
2
1, 3
WT
2 wpi
double
conditioning
lesion
J
WT
tKO+CL
WT+dCL
WT+GDNF
Axon Number Index
0.0
0.1
0.2
0.3
0.4
0.5
DREZ
0
100
200
300
400
500
Penetration into the CNS (um)
****
****
*
****
****
**
E, F, G, H
DH
VH
E
WT
DR
DH
GFP
CGRP
DAPI
GFP/CGRP
F
tKO+CL
G
WT+dCL
GFAP
H
WT+dCL
Laminin
I
WT+GDNF
GFP/GFAP

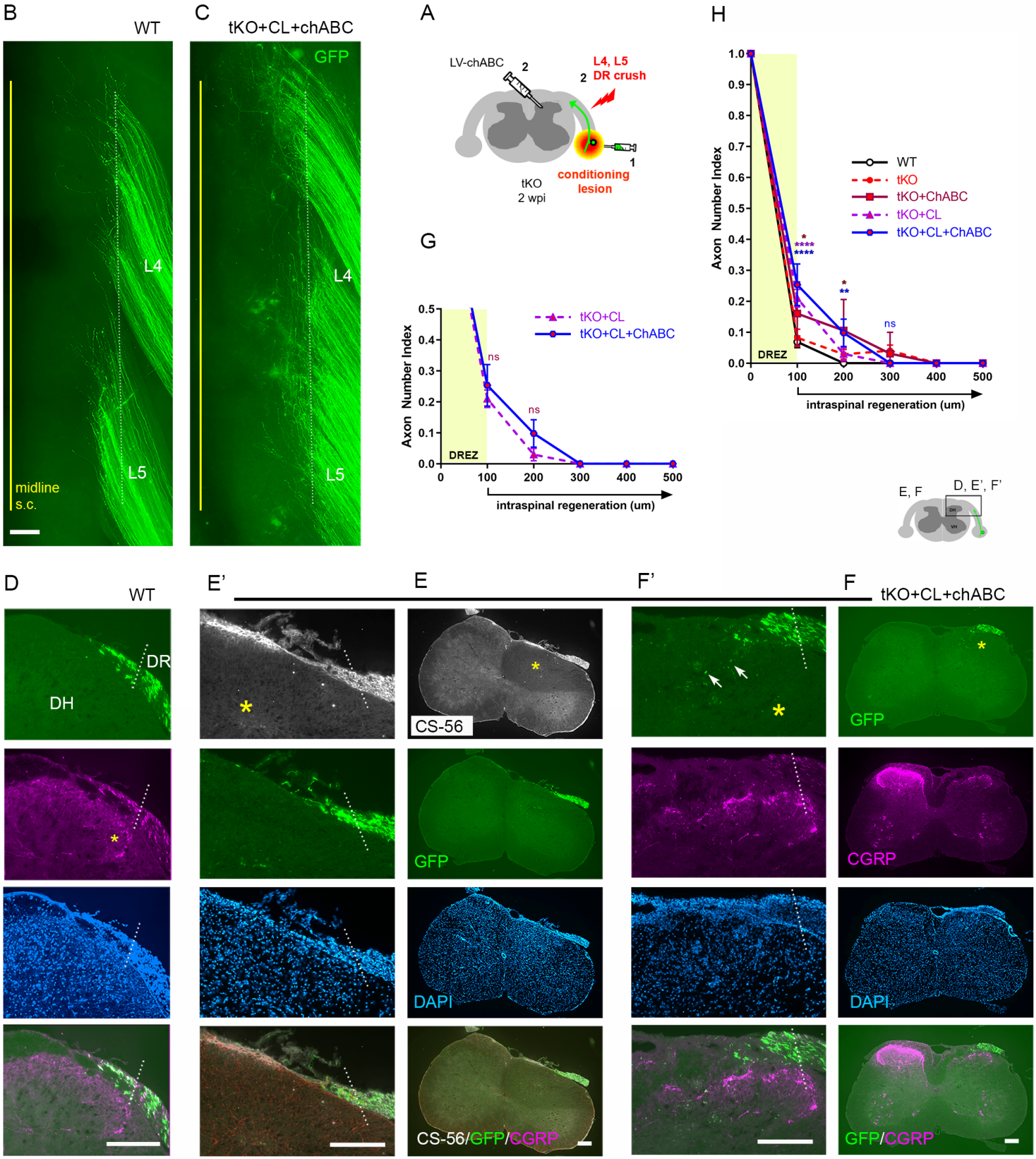
B
WT
C
tKO+CL+chABC
GFP
L4
L5
midline
s.c.
A
LV-chABC
2
2
L4, L5
DR crush
1
conditioning
lesion
tKO
2 wpi
G
Axon Number Index
tKO+CL
tKO+CL+ChABC
ns
ns
DREZ
intraspinal regeneration (um)
H
Axon Number Index
WT
tKO
tKO+ChABC
tKO+CL
tKO+CL+ChABC
DREZ
intraspinal regeneration (um)
E, F
D, E', F'
D
WT
DR
DH
E'
E
F'
F
tKO+CL+chABC
CS-56
GFP
CGRP
DAPI
CS-56/GFP/CGRP
GFP/CGRP

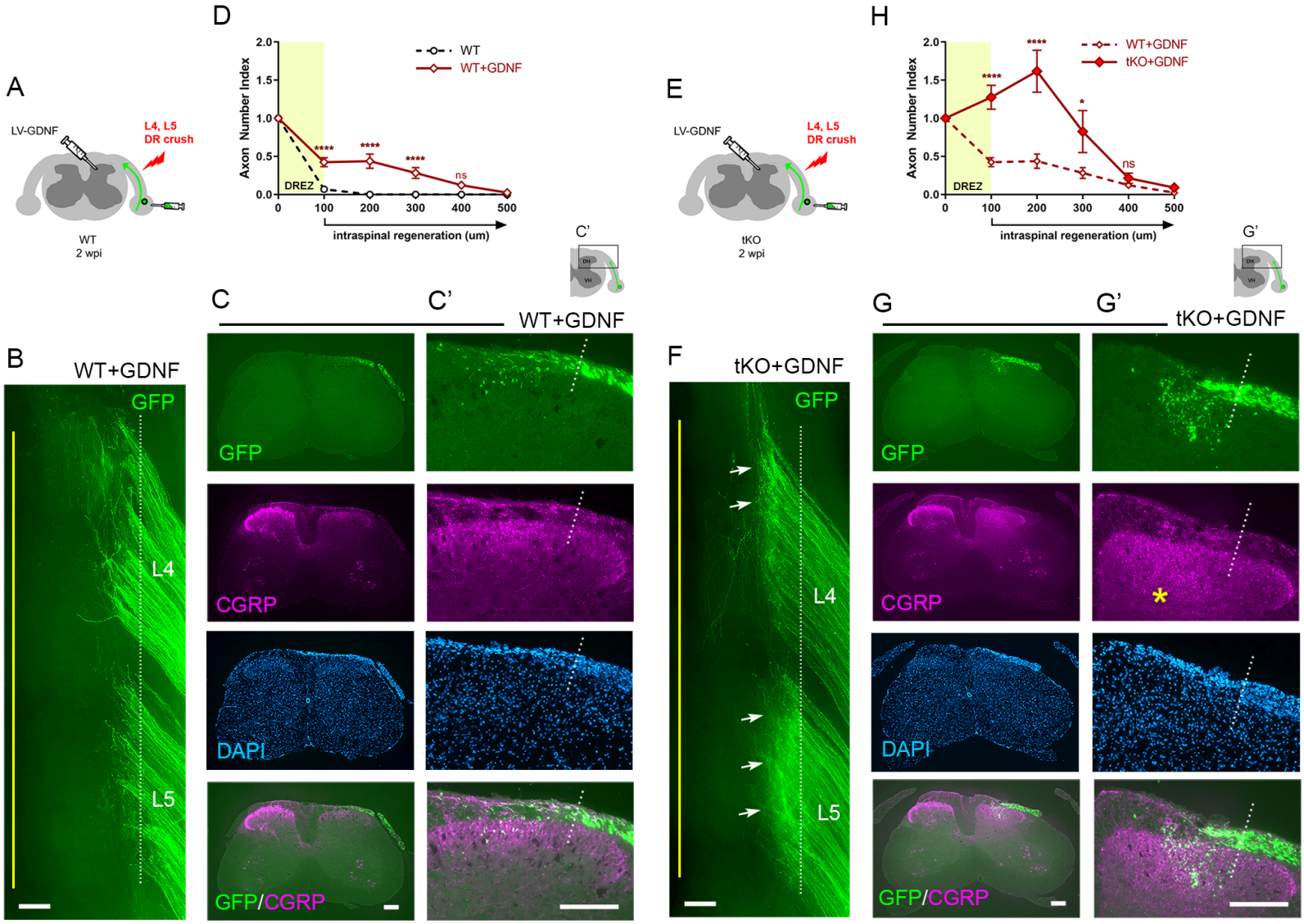
A
LV-GDNF
L4, L5
DR crush
WT
2 wpi
D
WT
WT+GDNF
Axon Number Index
DREZ
intraspinal regeneration (um)
****
ns
C'
B
WT+GDNF
GFP
L4
L5
C
C'
WT+GDNF
GFP
CGRP
DAPI
GFP/CGRP
E
LV-GDNF
L4, L5
DR crush
tKO
2 wpi
H
WT+GDNF
tKO+GDNF
Axon Number Index
DREZ
intraspinal regeneration (um)
****
*
ns
G'
F
tKO+GDNF
GFP
L4
L5
G
G'
tKO+GDNF
GFP
CGRP
DAPI
GFP/CGRP

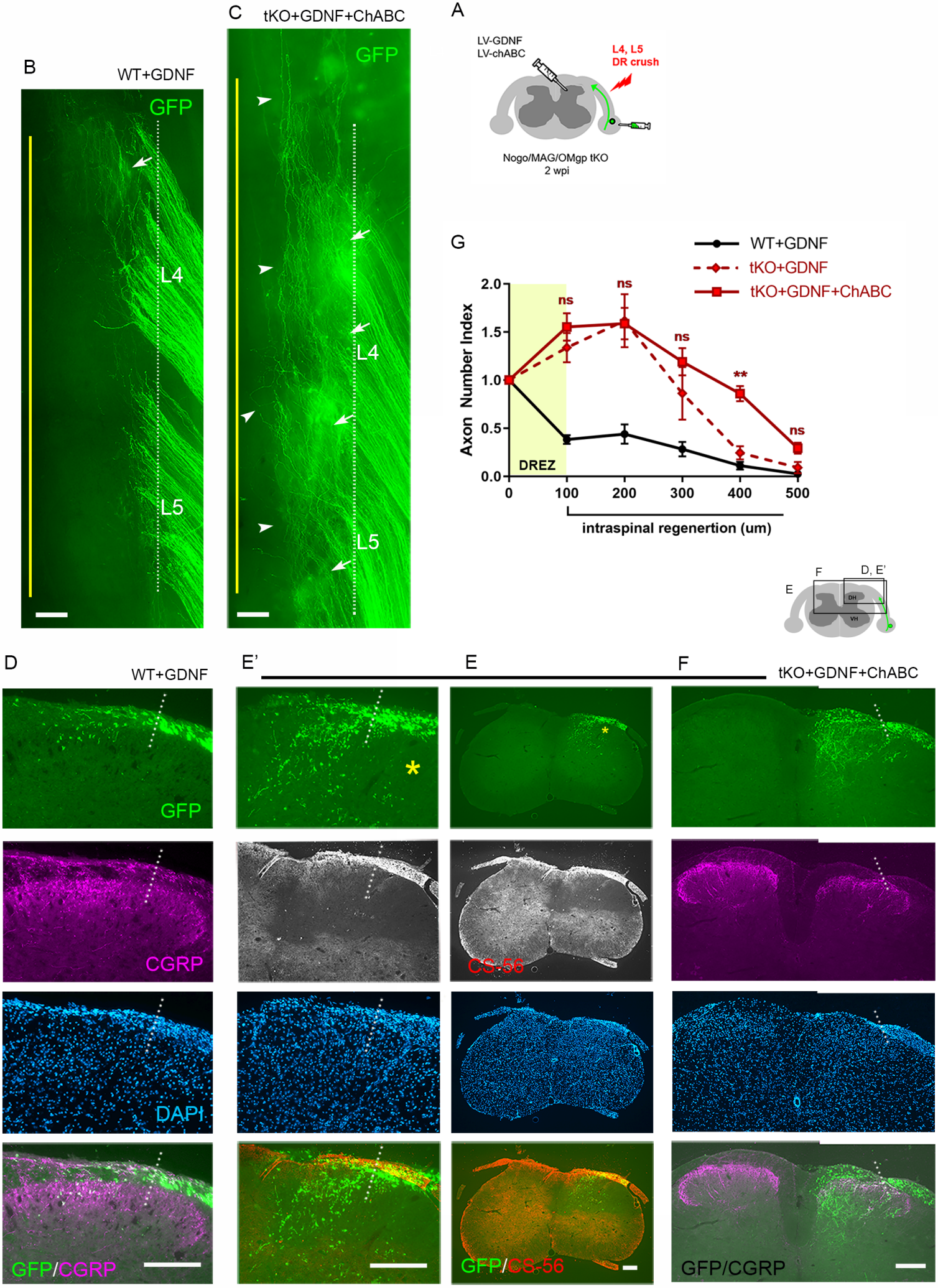
A
LV-GDNF
LV-chABC
L4, L5
DR crush
Nogo/MAG/OMgp tKO
2 wpi
B
WT+GDNF
GFP
L4
L5
C
tKO+GDNF+ChABC
GFP
L4
L5
G
WT+GDNF
tKO+GDNF
tKO+GDNF+ChABC
Axon Number Index
2.0
1.5
1.0
0.5
0.0
ns
ns
ns
**
ns
DREZ
0
100
200
300
400
500
intraspinal regenerion (um)
F
D, E'
E
DH
VH
D
WT+GDNF
E'
E
F
tKO+GDNF+ChABC
GFP
CGRP
CS-56
DAPI
GFP/CGRP
GFP/CS-56
GFP/CGRP